

CZECH TECHNICAL UNIVERSITY IN PRAGUE  
FACULTY OF NUCLEAR SCIENCES AND PHYSICAL ENGINEERING

## MASTER'S THESIS

ANYONS AND THEIR SIGNIFICANCE  
IN QUANTUM MECHANICS  
AND STATISTICAL PHYSICS

2011

VÁCLAV ZATLOUKAL

# Contents

<b>1</b>	<b>Introduction</b>	<b>3</b>
<b>2</b>	<b>Genesis and the basic properties of anyons</b>	<b>5</b>
2.1	Quantum statistics in $d$ dimensions . . . . .	6
2.1.1	Configuration spaces for identical particles . . . . .	6
2.1.2	Path integral quantization in two dimensions . . . . .	9
2.2	Quantum formalism for anyons . . . . .	11
2.2.1	Two-anyon problem . . . . .	13
2.3	Fractional statistics . . . . .	15
<b>3</b>	<b>Anyons in experiments</b>	<b>18</b>
3.1	Quantum Hall effect . . . . .	18
3.1.1	Electron gas confined to two dimensions . . . . .	19
3.1.2	Planar electron in a magnetic field . . . . .	21
3.1.3	Many-particle states . . . . .	26
3.1.4	Quasiparticles in the fractional QHE . . . . .	28
3.1.5	Hall plateaux . . . . .	31
3.2	High-temperature superconductivity . . . . .	32
<b>4</b>	<b>Propagation of anyons on the toric code</b>	<b>33</b>
4.1	Toric code – introduction . . . . .	33
4.2	Toric code Hamiltonian and anyonic excitations . . . . .	37
4.2.1	Stability of a quantum memory . . . . .	38
4.2.2	Anyonic statistics revealed . . . . .	39
4.2.3	Perturbation induced anyonic quantum walks . . . . .	40
4.3	Ladder lattice model . . . . .	42
4.3.1	One anyon walk . . . . .	45
4.4	Continuous-time quantum walks in one dimension . . . . .	48

4.4.1	Cyclic lattice . . . . .	48
4.4.2	Infinite line . . . . .	51
4.4.3	Cyclic lattice with disordered couplings . . . . .	54
4.5	Numerical results for one anyon walk on a periodic ladder lattice . . . . .	57
4.5.1	Regular disorder – delocalization . . . . .	60
4.5.2	Random disorder – localization . . . . .	61
<b>5</b>	<b>Conclusion</b>	<b>66</b>
<b>A</b>	<b>Braid group</b>	<b>67</b>
A.1	Representations of the braid group . . . . .	70

# Chapter 1

## Introduction

It is commonly accepted in physics that there are two kinds of particles in the three-dimensional space — bosons and fermions. In statistical physics, bosons obey the Bose-Einstein distribution law, while fermions are distributed among energy levels according to the Fermi-Dirac distribution. In quantum mechanics, they differ by the phase factor that the global wave function of a many-particle system acquires when two particles are exchanged. The phase factor is  $+1$  for bosons and  $-1$  for fermions.

The key concept in these considerations is the principle of indistinguishability of identical particles. No quantum mechanical observable can distinguish between two particle configurations that differ only by a permutation of identical particles. But what does the word “permutation” or “exchange” of identical particles actually mean? And how to understand the notion of “identicalness”, anyway. In 1977, Leinaas and Myrheim [1] took these questions seriously and found that whereas in three dimensions, indeed, only bosons and fermions should exist, the two-dimensional space offers a whole continuous family of possible quantum statistics. In two dimensions, one can consistently assign any phase factor  $e^{i\alpha}$  to reflect an exchange of two identical particles. Planar particles with these exotic statistics were named *anyons* by Frank Wilczek.

We dedicate the Chapter 2 to explaining the ideas of Leinaas and Myrheim and to formulating the basics of quantum mechanical description of anyons. The role of anyons in statistical physics is also discussed. There have been several attempts to generalize the bosonic and fermionic statistics, i.e. the number of particles that are allowed to occupy one quantum state. We present the work of Haldane [2], who generalized the Pauli exclusion principle in the way that the maximum number of particles that can occupy one quantum state is anywhere between 1 (fermions) and  $\infty$  (bosons). This so called *fractional statistics* is, however, found to be incompatible with anyons defined through the exotic exchange

phase  $e^{i\alpha}$  when confronted with thermodynamical results for an ideal gas of anyons [3].

In Chapter 3, the anyons are explored from the experimental point of view. We discuss how a two-dimensional system can be realized in practice and review the *quantum Hall effect* to show that the quasiparticles that appear in the *fractional* quantum Hall system exhibit exotic exchange statistics, i.e. that they are anyons [4]. Finally, we briefly overview the *high-temperature superconductivity*, a yet unexplained phenomenon, in which anyons were believed to take place as well. The experimental results, however, indicate that anyons are currently observed only in the fractional quantum Hall effect.

In the last chapter, Chapter 4, we wander into the field of *topological quantum computation*. We introduce the Kitaev's *toric code* [5], which is the most renowned topological quantum error correcting code. It can serve as a quantum memory, robustness of which is achieved on the physical (hardware) level. Anyonic excitations occur on the toric code as local errors and if they propagate far enough, they cause logical errors, i.e. the quantum information, stored in the quantum memory, is lost. Our objective is to investigate how the nontrivial exchange statistics affects the *continuous-time quantum walk* of anyons on the toric code. Especially, we would like to know whether a certain type of disorder in the system causes *Anderson localization* [6] to take place as argued by Wootton and Pachos [7].

## Chapter 2

# Genesis and the basic properties of anyons

At the beginning of this chapter we focus on the theory of identical particles in a general spatial dimension  $d$ . We show how the topology of configuration spaces of systems of identical particles depend on the spatial dimension and what consequences a nontrivial topology, expressed in terms of the fundamental group of a configuration space, has for the concept of quantum statistics. Whereas in three and more dimensions only bosonic and fermionic exchange statistics exist, in a two dimensional space the infinite connectedness of the configuration space allows for much greater diversity. The phase factor that a wave function acquires upon an exchange of two particles doesn't have to be merely the bosonic  $+1$  or the fermionic  $-1$ , but can be, in principle, an arbitrary complex unit. The particles in two dimensions are called anyons.

In the next part we formulate the Lagrangian and the Hamiltonian that incorporate the general anyonic statistics. Based on the solution of the two-anyon problem, we argue that free anyons (meaning without a direct force between them) exhibit a repulsive interaction (similar in nature, but weaker than fermions) arising purely from their exchange statistics.

In statistical mechanics, bosons and fermions are described by distinct statistical distributions over the energy states that they obey in thermal equilibrium — Bose-Einstein and Fermi-Dirac distributions. The last section presents a generalization of these two possibilities, the fractional statistics. The connection between anyons and the fractional statistics is, however, not as straightforward. In fact, those two seem to be rather different concepts — anyons don't obey the fractional statistics.

## 2.1 Quantum statistics in $d$ dimensions

Before we come to a proper discussion about the statistics, it is worth clarifying what exactly one means by quantum statistics. In most textbooks on statistical mechanics, the term “quantum statistics” refers to the phase picked up by a wave function when two identical particles are interchanged, i.e. under the permutation of the particles. One usually writes

$$\psi(\mathbf{x}_2, \mathbf{x}_1) = e^{i\alpha} \psi(\mathbf{x}_1, \mathbf{x}_2) . \quad (2.1)$$

But this is slightly misleading and has been correctly criticized in literature [8]. If the particles are strictly identical then the word “permutation” has no physical meaning since a given configuration and the one obtained by the permutation of particle coordinates are merely two different ways of describing the *same* particle configuration. The two quantities in equation (2.1) have no separate meaning and the equation therefore at most reflects a redundancy in the notation.

The origin of the trouble lies in the introduction of the particle indices which brings elements of non-observable character into the theory and makes the discussion more obscure. The term quantum statistics actually refers to the phase that arises when two particles are adiabatically transported giving rise to the exchange. The principle of indistinguishability of identical particles plays the central role and it has, as we shall see, profound physical consequences.

### 2.1.1 Configuration spaces for identical particles

Following Khare [3] and Leinaas and Myrheim [1], let us enquire about the configuration space of a system of identical particles. In statistical mechanics one normally considers the full phase space, but it turns out that the configuration space is enough for this discussion. Suppose one particle space is  $X$ . Then what is the configuration space of  $N$  identical particles? The naive answer is  $X^N$ , which, even though is true locally, is not correct globally. Since the particles are strictly identical, there is no distinction between the points in  $X^N$  that differ only in the ordering of the particle coordinates.

For example, take the point

$$\mathbf{x} = (\mathbf{x}_1, \mathbf{x}_2, \dots, \mathbf{x}_N) \quad (2.2)$$

in  $X^N$ , where  $\mathbf{x}_i \in X$  for  $i = 1, 2, \dots, N$ . Now consider another point  $\mathbf{x}'$  in  $X^N$  which is obtained from  $\mathbf{x}$  by the permutation  $p$  of the particle indices, i.e.

$$\mathbf{x}' = p(\mathbf{x}) = (\mathbf{x}_{p(1)}, \dots, \mathbf{x}_{p(N)}) . \quad (2.3)$$

Clearly, both  $\mathbf{x}$  and  $\mathbf{x}'$  describe the *same* physical configuration of the system. Thus the true configuration space of the  $N$ -particle system is not the Cartesian product  $X^N$ , but it is the quotient space  $X^N/S_N$  which is obtained by identifying the points of  $X^N$  that represent the same physical configuration, i.e. it is obtained by “dividing out” the action of the symmetric (or permutation) group  $S_N$ . Note that  $S_N$  is a discrete and indeed finite transformation group acting in  $X^N$ . As a result, the space  $X^N/S_N$  is locally diffeomorphic to  $X^N$  except at the points

$$\Delta = \{(\mathbf{x}_1, \dots, \mathbf{x}_N) \in X^N \mid \mathbf{x}_i = \mathbf{x}_j \text{ for some } i \neq j\} , \quad (2.4)$$

where two or more particles occupy the same position in  $X$ . For convenience, we remove the points of  $\Delta$  from our configuration space<sup>1</sup>, i.e. the configuration space of  $N$  identical particles becomes

$$(X^N \setminus \Delta)/S_N . \quad (2.5)$$

Since the spaces  $X^N \setminus \Delta$  and  $(X^N \setminus \Delta)/S_N$  are locally diffeomorphic, they are equivalent on the classical level. However, on the quantum level global properties of the configuration space are of deep physical significance as we shall see later when we will path-integral quantize the system of identical particles.

Let us now study in detail the configuration space  $(X^N \setminus \Delta)/S_N$  under the assumption that the one particle configuration space  $X$  is the  $d$ -dimensional Euclidean space  $\mathbb{R}^d$ ,  $d = 1, 2, 3, \dots$ . Let us take, for simplicity, the two particle case ( $N = 2$ ), i.e. the space  $((\mathbb{R}^d \times \mathbb{R}^d) \setminus \Delta)/S_2$ . Using the center-of-mass coordinate

$$\mathbf{x}_{c.m.} = \frac{\mathbf{x}_1 + \mathbf{x}_2}{2} \quad (2.6)$$

and the relative coordinate

$$\mathbf{x}_r = \mathbf{x}_2 - \mathbf{x}_1 , \quad (2.7)$$

where  $\mathbf{x}_1, \mathbf{x}_2 \in \mathbb{R}^d$  are the coordinates of the individual particles, we can see that removing the set of coincidence  $\Delta$  from our configuration space is expressed by the condition  $\mathbf{x}_r \neq \mathbf{0}$ . The identification of the points  $(\mathbf{x}_1, \mathbf{x}_2)$  and  $(\mathbf{x}_2, \mathbf{x}_1)$  corresponds to identifying the points  $(\mathbf{x}_{c.m.}, \mathbf{x}_r)$  and  $(\mathbf{x}_{c.m.}, -\mathbf{x}_r)$ . Therefore the configuration space of two identical particles reads

$$((\mathbb{R}^d \times \mathbb{R}^d) \setminus \Delta)/S_2 = \mathbb{R}^d \times (S^{d-1}/S_2) \times (0, +\infty) , \quad (2.8)$$

---

<sup>1</sup>Whether or not two particles can simultaneously occupy the same position is not a question we wish to settle here. We are only saying that by excluding the points of coincidence from the configuration space, the resulting topology leads to meaningful physical results without any further assumptions.

where  $S^{d-1}/S_2$  is the  $(d-1)$ -dimensional sphere with diametrically opposite points identified, i.e in fact the real projective space  $\mathbb{R}P^{d-1}$ .

To reveal the global topological properties of the configuration spaces  $\mathbb{R}^d \times (S^{d-1}/S_2) \times (0, +\infty)$  of two identical particles, we will find their fundamental group<sup>2</sup>  $\pi_1$  for any dimension  $d$ . (The fundamental group plays a key role in the path integral quantization in topologically non-trivial spaces.) We make use of the fact that for any two topological spaces  $A$  and  $B$

$$\pi_1(A \times B) = \pi_1(A) \otimes \pi_1(B) , \quad (2.9)$$

where "  $\times$  " is the Cartesian product of two sets while "  $\otimes$  " stands for the direct product of groups. Thus

$$\pi_1(\mathbb{R}^d \times (S^{d-1}/S_2) \times (0, +\infty)) = \pi_1(\mathbb{R}^d) \otimes \pi_1(S^{d-1}/S_2) \otimes \pi_1((0, +\infty)) = \pi_1(S^{d-1}/S_2) , \quad (2.10)$$

since both  $\mathbb{R}^d$  and  $(0, +\infty)$  are simply connected topological spaces.

There are several possibilities (follow the figure 2.1).

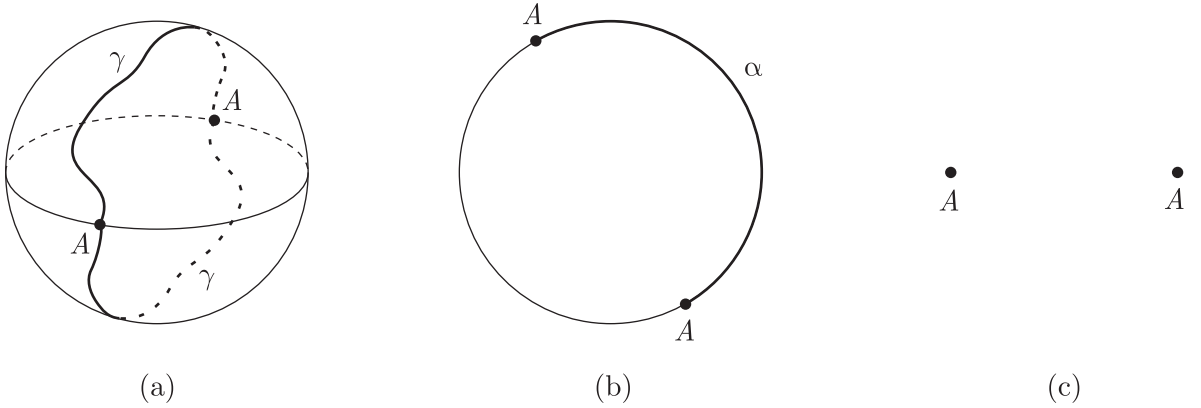


Figure 2.1: (a) The topological space  $S^{d-1}/S_2$  for  $d \geq 3$  is doubly connected, i.e.  $\pi_1(S^{d-1}/S_2) = \mathbb{Z}_2$ . The path  $\gamma$  represents homotopically nontrivial paths;  $\gamma^2$  is, however, homotopically trivial. (b) The space  $S^1/S_2$  is infinitely connected,  $\pi_1(S^1/S_2) = \mathbb{Z}$ . The fundamental group is generated by the path  $\alpha$ . (c) The space  $S^0/S_2$  is trivial (it is a single point), thus its fundamental group is trivial as well.

For  $d \geq 3$ :

$$\pi_1(S^{d-1}/S_2) = \mathbb{Z}_2 . \quad (2.11)$$

<sup>2</sup>For an introduction into this topic see for example [9].

The only path (up to a homotopy) that is not contractible to a single point is the one that terminates at the point of  $S^{d-1}$  antipodal to the point of its origin. (In Figure 2.1(a) such a path is denoted  $\gamma$ .) If, however, we travel this path twice then the resulting path  $\gamma \cdot \gamma$  ( $\gamma$  followed by  $\gamma$ ) can be continuously shrunk to a point as it forms a closed path on the sphere  $S^{d-1}$ . Notice that  $\gamma$  represents one exchange of the two identical particles and  $\gamma \cdot \gamma$  represents two such exchanges. If the two particles were not identical, the fundamental group would be the one of a  $(d-1)$ —dimensional sphere, i.e. it would be trivial.

For  $d = 2$ :

$$\pi_1(S^1/S_2) = \mathbb{Z} . \quad (2.12)$$

The path  $\alpha$  (see Fig.2.1(b)) is not contractible to a point and paths of the form  $\alpha^n, n \in \mathbb{Z}$  are all homotopy inequivalent. The configuration space of two identical particles in a plane is multiply connected and therefore will admit a richer exchange statistics. If the two particles were not identical, the fundamental group would be the one of a circle, i.e. again  $\mathbb{Z}$ .

For  $d = 1$ :

$$\pi_1(S^0/S_2) \text{ is trivial.} \quad (2.13)$$

This is an obvious result since we are computing the fundamental group of a single point. If the two particles were not identical, their configuration space would be disconnected.

It is problematic to define the exchange statistics in one dimension as particles cannot be exchanged without their passing through one another. As a result, the intrinsic statistics is inextricably mixed up with local interactions.

In the general problem of  $N$  identical particles one has to find the fundamental group of the space  $((\mathbb{R}^d)^N \setminus \Delta)/S_N$ . This problem was solved in [10, 11] with the results

$$\pi_1(((\mathbb{R}^d)^N \setminus \Delta)/S_N) = B_N \quad \text{for } d = 2 , \quad (2.14)$$

$$\pi_1(((\mathbb{R}^d)^N \setminus \Delta)/S_N) = S_N \quad \text{for } d \geq 3 , \quad (2.15)$$

where  $B_N$  is the *braid group* of  $N$  objects (strings) while  $S_N$  is the permutation group. It turns out that whereas there are only two one dimensional representations of the permutation group  $S_N$  (the trivial one and the alternating one, corresponding respectively to the bosonic and the fermionic statistics), the braid group  $B_N$  admits a continuous family of one dimensional representations. A brief braid group introduction is given in Appendix A.

## 2.1.2 Path integral quantization in two dimensions

We have seen that whereas the configuration space of  $N$  identical particles in three and higher space dimensions is doubly connected, it is multiply connected in two dimensions.

This fact has profound consequences when we quantize the system of identical particles. To quantize a system with topologically nontrivial configuration space it is convenient to use the path integral formulation.

According to Feynman [12], the transition amplitude from the configuration  $|\mathbf{x}_i\rangle$  at time  $t_i$  to the configuration  $|\mathbf{x}_f\rangle$  at  $t_f$  is given by

$$\langle \mathbf{x}_f, t_f | \mathbf{x}_i, t_i \rangle = N \sum_{\mathbf{x}(t)} \exp \left( \frac{i}{\hbar} S[\mathbf{x}(t)] \right) , \quad (2.16)$$

where  $N$  is a normalization constant, the sum is taken over all paths in the configuration space  $\mathbf{x}(t)$ ,  $t \in [t_i, t_f]$  with  $\mathbf{x}(t_i) = \mathbf{x}_i$  and  $\mathbf{x}(t_f) = \mathbf{x}_f$ , and the action  $S$  is evaluated along a path  $\mathbf{x}(t)$  through the prescription

$$S[\mathbf{x}(t)] = \int_{t_i}^{t_f} L(\mathbf{x}(t), \dot{\mathbf{x}}(t)) dt . \quad (2.17)$$

In configuration spaces with nontrivial fundamental group  $\pi_1$  the prescription (2.16) generalizes, according to DeWitt [13], to the form

$$\langle \mathbf{x}_f, t_f | \mathbf{x}_i, t_i \rangle = N \sum_{[\gamma] \in \pi_1(X)} \chi([\gamma]) \sum_{\mathbf{x}(t) \in [\gamma]} \exp \left( \frac{i}{\hbar} S[\mathbf{x}(t)] \right) , \quad (2.18)$$

i.e. each path is weighted by an extra factor  $\chi([\gamma])$ , which depends on the homotopy class that the path belongs to. The factors  $\chi([\gamma])$  form a scalar<sup>3</sup> unitary representation of the fundamental group of the configuration space,

$$\chi([\gamma_1][\gamma_2]) = \chi([\gamma_1])\chi([\gamma_2]) . \quad (2.19)$$

In three or higher spatial dimensions there are two scalar representations of the fundamental group  $S_N$ . An exchange of two identical particles can introduce a factor of either +1 or -1 for bosons or fermions, respectively.

There are more possibilities in two spatial dimensions, where the fundamental group of the configuration space is the braid group  $B_N$ . In fact, it is possible to consistently assign *any* value

$$\chi([\gamma]) = e^{i\alpha} , \quad \alpha \in [0, 2\pi] \quad (2.20)$$

to the phase arising due to the exchange of two particles. Particles in two dimensional space are called *anyons* and their characterization  $\alpha$  is called the *exchange parameter*. Bosons and fermions are special cases of anyons with  $\alpha = 0$  and  $\alpha = \pi$ , respectively.

---

<sup>3</sup>In more general theories also higher-dimensional representations are considered.

One can generalize the concept of anyons for the case of multicomponent wave functions. The exchange parameter is then allowed to take values in unitary matrices, which carry higher dimensional representations of the braid group. Anyons whose prefactor are noncommutative are called *non-Abelian*. However, we shall only encounter so called *Abelian* anyons with the exchange parameter a genuine complex unit  $e^{i\alpha}$ .

There is a connection between the exchange statistics of two (or more) particles and the spin of an individual particle — the *spin-statistics theorem*.<sup>4</sup> It states that bosons, whose global wave function acquires +1 when two particles are exchanged, have integer spin, whereas fermions, whose global wave function acquires  $-1$  when two particles are exchanged, have half-integer spin. The restriction on the values of spin is a consequence of the commutation relations

$$[S_i, S_j] = i\hbar\varepsilon_{ijk}S_k \quad (2.21)$$

for the spin operators  $S_x$ ,  $S_y$  and  $S_z$  in three dimensions. In two dimensions, however, there is only one direction of rotation and therefore only one spin operator  $S$ . There is no restriction on the eigenvalues of  $S$  as the algebra generated by  $S$  is commutative. This is in consistency with the fact that in two dimensions there are no restrictions on the possible values of the statistical exchange phase  $e^{i\alpha}$ .

## 2.2 Quantum formalism for anyons

We will formulate the basics of quantum mechanics of anyons and later examine the two-body problem of free anyons.

The Lagrangian for  $N$  ordinary identical particles with mass  $M$  and an interaction potential  $V$  is

$$L_0 = \frac{M}{2} \sum_{j=1}^N \dot{\mathbf{x}}_j^2 - V(\mathbf{x}_1, \dots, \mathbf{x}_N) . \quad (2.22)$$

To convert the ordinary particles into anyons we introduce the “statistical interaction” term and obtain the anyonic Lagrangian

$$L = L_0 + \frac{\alpha\hbar}{\pi} \sum_{r>s} \frac{d}{dt} \theta(\mathbf{x}_r - \mathbf{x}_s) , \quad (2.23)$$

where  $\alpha$  is the anyonic exchange parameter and  $\theta(\mathbf{x}_r - \mathbf{x}_s)$  is the angle between the vector  $\mathbf{x}_r - \mathbf{x}_s$  and the  $x$  axis.

---

<sup>4</sup>It is proved in the framework of quantum field theory [14]. In quantum mechanics, the spin-statistics “theorem” must be *postulated*.

The role of the statistical interaction term is most easily explained within the path integral formulation. For simplicity, let us consider two particles evolving from the initial configuration  $|\mathbf{x}_1^i, \mathbf{x}_2^i\rangle$  at time  $t_i$  to the final configuration  $|\mathbf{x}_1^f, \mathbf{x}_2^f\rangle$  at time  $t_f$  and calculate the action  $S \equiv S[\mathbf{x}_1(t), \mathbf{x}_2(t)]$  along a particular path  $(\mathbf{x}_1(t), \mathbf{x}_2(t))$ ,

$$S = \int_{t_i}^{t_f} L_0(\mathbf{x}_1(t), \mathbf{x}_2(t)) dt + \frac{\alpha \hbar}{\pi} \Delta\theta \quad (2.24)$$

with  $\Delta\theta \equiv \theta(\mathbf{x}_2^f - \mathbf{x}_1^f) - \theta(\mathbf{x}_2^i - \mathbf{x}_1^i)$ . The contribution to the path integral associated with this trajectory is the phase

$$e^{\frac{i}{\hbar} S} = e^{i\alpha \frac{\Delta\theta}{\pi}} e^{\frac{i}{\hbar} \int L_0 dt} . \quad (2.25)$$

We can see that when the angle  $\theta(\mathbf{x}_2 - \mathbf{x}_1)$  changes by  $\Delta\theta = \pi$ , i.e. when the two particles are interchanged, the extra phase  $e^{i\alpha}$  reproduces the exchange phase between the anyons with the exchange parameter  $\alpha$  (2.20).

Comments are in order. (1) Since the statistical interaction term

$$\frac{\alpha \hbar}{\pi} \sum_{r>s} \frac{d}{dt} \theta(\mathbf{x}_r - \mathbf{x}_s) \quad (2.26)$$

is a total time derivative, it does not contribute to classical equations of motion. Anyonic statistics is purely quantum effect with no classical analogue. (2) Anyons violate discrete symmetries of parity  $\mathcal{P} : (x, y) \rightarrow (x, -y)$  and time reversal  $\mathcal{T} : t \rightarrow -t$  as

$$\frac{d\theta}{dt} \xrightarrow{\mathcal{P}} -\frac{d\theta}{dt} , \quad \frac{d\theta}{dt} \xrightarrow{\mathcal{T}} -\frac{d\theta}{dt} . \quad (2.27)$$

In order to proceed from the Lagrangian (2.23) to the Hamilton's formalism we'll find the canonical momenta  $\mathbf{p}_m = \frac{\partial L}{\partial \dot{\mathbf{x}}_m}$ . First, we note that

$$\frac{d\theta(\mathbf{x})}{dt} = \frac{d}{dt} \left( \arctan \frac{x^2}{x^1} \right) = \frac{\dot{x}^2 x^1 - \dot{x}^1 x^2}{\|\mathbf{x}\|^2} = -\varepsilon_{jk} \frac{\dot{x}^j x^k}{\|\mathbf{x}\|^2} \quad (2.28)$$

so that

$$\frac{\partial}{\partial \dot{x}_m^j} \sum_{r>s} \frac{d}{dt} \theta(\mathbf{x}_r - \mathbf{x}_s) = - \sum_{s \neq m} \varepsilon_{jk} \frac{x_m^k - x_s^k}{\|\mathbf{x}_m - \mathbf{x}_s\|^2} . \quad (2.29)$$

Hence, the canonical momenta are

$$\mathbf{p}_m = \frac{\partial L}{\partial \dot{\mathbf{x}}_m} = M \dot{\mathbf{x}}_m + \frac{\alpha \hbar}{\pi} \frac{\partial}{\partial \dot{\mathbf{x}}_m} \sum_{r>s} \frac{d}{dt} \theta(\mathbf{x}_r - \mathbf{x}_s) = M \dot{\mathbf{x}}_m + e \mathbf{C}(\mathbf{x}_m) , \quad (2.30)$$

where

$$C_j(\mathbf{x}_m) = \frac{\Phi}{2\pi} \sum_s \partial_j \theta(\mathbf{x}_m - \mathbf{x}_s) = -\frac{\Phi}{2\pi} \sum_{s \neq m} \varepsilon_{jk} \frac{x_m^k - x_s^k}{\|\mathbf{x}_m - \mathbf{x}_s\|^2} \quad (2.31)$$

is the *Chern-Simons* gauge potential and the constants  $e$  and  $\Phi$ , satisfying  $e\Phi = 2\alpha\hbar$ , are introduced to emphasize the analogy between  $\mathbf{C}(\mathbf{x})$  and the electromagnetic potential  $\mathbf{A}(\mathbf{x})$ .<sup>5</sup> Yet, the Chern-Simons potential  $\mathbf{C}(\mathbf{x})$  is only a fictitious, purely mathematical device that realizes the anyonic statistics.

The Hamiltonian is given by the Legendre transform,

$$H = \sum_{m=1}^N \mathbf{p}_m \cdot \dot{\mathbf{x}}_m - L = \frac{1}{2M} \sum_{m=1}^N (\mathbf{p}_m - e\mathbf{C}(\mathbf{x}_m))^2 + V(\mathbf{x}_1, \dots, \mathbf{x}_N) . \quad (2.32)$$

We may regard anyons as ordinary bosons carrying the Chern-Simons charge  $e$  and flux  $\Phi$ .

### 2.2.1 Two-anyon problem

Let us consider an example of two noninteracting anyons. Noninteracting in the sense that there is no potential term. On the other hand, being anyons, they will influence each other by the statistical interaction.

The Hamiltonian is given by

$$H = \frac{1}{2M} (\mathbf{p}_1 - e\mathbf{C}(\mathbf{x}_1))^2 + \frac{1}{2M} (\mathbf{p}_2 - e\mathbf{C}(\mathbf{x}_2))^2 \quad (2.33)$$

with

$$C_j(\mathbf{x}_1) = -\frac{\Phi}{2\pi} \varepsilon_{jk} \frac{x_1^k - x_2^k}{\|\mathbf{x}_1 - \mathbf{x}_2\|^2} = -C_j(\mathbf{x}_2) . \quad (2.34)$$

In the center-of-mass coordinate system

$$\mathbf{R} = \frac{\mathbf{x}_1 + \mathbf{x}_2}{2} , \quad \mathbf{r} = \mathbf{x}_1 - \mathbf{x}_2 \quad (2.35)$$

the momentum operators  $\mathbf{p}_1 = -i\hbar \frac{\partial}{\partial \mathbf{x}_1}$  and  $\mathbf{p}_2 = -i\hbar \frac{\partial}{\partial \mathbf{x}_2}$  read

$$\mathbf{p}_1 = \frac{\mathbf{p}_R}{2} + \mathbf{p}_r , \quad \mathbf{p}_2 = \frac{\mathbf{p}_R}{2} - \mathbf{p}_r \quad (2.36)$$

and the Hamiltonian separates into two parts

$$\begin{aligned} H &= \frac{1}{2M} \left( \frac{\mathbf{p}_R}{2} + \mathbf{p}_r - e\mathbf{C}(\mathbf{x}_1) \right)^2 + \frac{1}{2M} \left( \frac{\mathbf{p}_R}{2} - \mathbf{p}_r + e\mathbf{C}(\mathbf{x}_1) \right)^2 \\ &= \frac{\mathbf{p}_R^2}{4M} + \frac{(\mathbf{p}_r - e\mathbf{C}(\mathbf{x}_1))^2}{M} \equiv H_R + H_r . \end{aligned} \quad (2.37)$$

---

<sup>5</sup> In electromagnetism, a particle with charge  $q$  having passed around an infinitely long solenoid with magnetic flux  $\phi$  experiences a phase shift

$$e^{\frac{i}{\hbar} q \oint \mathbf{A} d\mathbf{x}} = e^{\frac{i}{\hbar} q \phi} .$$

It is known as the *Aharonov-Bohm effect* [15].

The center-of-mass Hamiltonian  $H_R$ , which is independent of the statistical parameter  $\alpha$ , describes a free particle and its eigenstates are plane waves.

We analyze the relative Hamiltonian  $H_r$  in polar coordinates. Since

$$\mathbf{C}(\mathbf{x}_1) = \frac{\Phi}{2\pi} \nabla \theta(\mathbf{r}) = \frac{\Phi}{2\pi} \frac{1}{r} (-\sin \theta, \cos \theta) , \quad (2.38)$$

after some calculations we arrive at

$$H_r = -\frac{\hbar^2}{M} \left[ \frac{1}{r} \frac{\partial}{\partial r} \left( r \frac{\partial}{\partial r} \right) + \frac{1}{r^2} \left( \frac{\partial}{\partial \theta} + i \frac{\alpha}{\pi} \right)^2 \right] . \quad (2.39)$$

Using the factorization ansatz for the wave function,  $\psi(r, \theta) = A(\theta)B(r)$ , the angular equation

$$\left( \frac{\partial}{\partial \theta} + i \frac{\alpha}{\pi} \right)^2 A(\theta) = \lambda A(\theta) \quad (2.40)$$

is obtained. Since we regard the two anyons as bosons interacting via the statistical interaction, the boundary condition on the eigenfunction  $A(\theta)$  is

$$A(\theta + \pi) = A(\theta) , \quad (2.41)$$

hence

$$A_l(\theta) = e^{il\theta} , \quad l = 0, \pm 2, \pm 4, \dots , \quad \lambda_l = - \left( l + \frac{\alpha}{\pi} \right)^2 . \quad (2.42)$$

The eigenvalues  $\lambda_l$  are non-degenerate except for two cases:  $\alpha = 0$  (bosons) and  $\alpha = \pi$  (fermions).

On substituting  $A_l(\theta)$  to the time-independent Schrödinger equation  $H_r \psi = E \psi$  we obtain the radial equation

$$-\frac{\hbar^2}{M} \left[ \frac{1}{r} \frac{d}{dr} \left( r \frac{d}{dr} \right) + \frac{\lambda_l}{r^2} \right] B(r) = E B(r) . \quad (2.43)$$

Solutions to this equation are the Bessel functions of the first kind,

$$B(r) = J_{\sqrt{-\lambda_l}}(kr) = J_{|l + \frac{\alpha}{\pi}|}(kr) , \quad E = \frac{k^2 \hbar^2}{M} , \quad (2.44)$$

which behave at  $r \rightarrow 0$  as

$$J_{|l + \frac{\alpha}{\pi}|}(kr) \approx \frac{1}{\Gamma(|l + \frac{\alpha}{\pi}| + 1)} \left( \frac{kr}{2} \right)^{|l + \frac{\alpha}{\pi}|} \sim r^{|l + \frac{\alpha}{\pi}|} . \quad (2.45)$$

We observe that two particles can come close together, for the wave function this means

$$|\psi(r \rightarrow 0, \theta)|^2 = |B(r \rightarrow 0)|^2 \neq 0 , \quad (2.46)$$

only if  $\alpha = 0$  (bosons) and  $l = 0$ . For  $\alpha > 0$  there is a centrifugal barrier that prevents the particles from occupying the same position. Apart from bosons, all other particles ( $0 < \alpha \leq \pi$ ) satisfy some kind of Pauli exclusion principle. The repulsion grows with increasing exchange parameter  $\alpha$ . In this sense, anyons behave like bosons with extra repulsion interaction or fermions with extra attractive interaction.

Quantum mechanics of interacting anyons has been studied in literature [3]. While two-anyon problems (oscillator potential, Coulomb field) can be solved, troubles arise when we consider three and more anyons, since we can no longer take advantage of the center of mass separation and the polar coordinate system.

## 2.3 Fractional statistics

In statistical mechanics, the particle statistics is described by the Pauli exclusion principle rather than by a phase factor that the global wave function acquires upon an exchange of particles. The Bose-Einstein statistics allows any number of particles (bosons) to occupy a given quantum state, whereas the Fermi-Dirac statistics allows only zero or one particle (fermions). These notions of exclusion statistics can be introduced in any spatial dimension (for example, two).

In 1991 Haldane [2] introduced the concept of *fractional exclusion statistics* generalizing the Pauli exclusion principle. He defined the statistics  $g$  of a particle by

$$g = \frac{d_N - d_{N+\Delta N}}{\Delta N}, \quad (2.47)$$

where  $N$  is the number of particles and  $d_N$  is the dimension of one-particle Hilbert space when other  $N - 1$  particles are kept fixed. In particular, for  $\Delta N = 1$  we can see that  $g = d_N - d_{N+1}$  denotes the number of quantum states that are filled by one extra particle in the system. Here, however,  $g$  is not required to be an integer. For bosons  $g_B = 0$ , for fermions  $g_F = 1$  and for anyons (if applicable) we would expect something in between.

On the basis of (2.47) Haldane proposed a formula for the number of many-body states of  $N$  identical particles occupying a group of  $p$  quantum states,

$$W = \frac{[p + (N - 1)(1 - g)]!}{N![p - gN - (1 - g)]!}. \quad (2.48)$$

The factorials, of course, need to be considered in a generalized sense of  $\Gamma$  functions. For bosons and fermions this reproduces the well known formulas

$$W_B = \frac{(p + N - 1)!}{N!(p - 1)!} \quad \text{and} \quad W_F = \frac{p!}{N!(p - N)!}. \quad (2.49)$$

When there are several  $p$ -fold degenerate energy levels  $\varepsilon_j$  with  $n_j$  particles in each of them, the number of microstates of the system

$$\Omega = \prod_j \frac{[p + (n_j - 1)(1 - g)]!}{n_j! [p - gn_j - (1 - g)]!} \quad (2.50)$$

determines the statistical entropy

$$S = k_B \ln \Omega . \quad (2.51)$$

Maximizing the entropy  $S$  as a function of the occupation numbers  $n_j$  and with the constraints on the total energy and the number of particles,

$$E = \sum_j n_j \varepsilon_j \quad , \quad N = \sum_j n_j \quad , \quad (2.52)$$

we obtain the least biased occupation numbers  $\bar{n}_j = \frac{n_j}{p}$ , i.e. the average number of particles occupying one quantum state in the  $j$ -th energy level. The calculation is done in [3], chapter 5, with the result

$$\bar{n}_j = \frac{1}{\omega(\xi_j) + g} \quad , \quad (2.53)$$

where  $\xi_j \equiv e^{\beta(\varepsilon_j - \mu)}$ ,  $\beta = \frac{1}{kT}$  is the inverse temperature,  $\mu$  is the chemical potential and the function  $\omega(\xi_j)$  satisfies the equation

$$\omega(\xi_j)^g (1 + \omega(\xi_j))^{1-g} = \xi_j . \quad (2.54)$$

For the particular cases  $g = 0$  and  $g = 1$  we immediately recover the familiar formulas for Bose-Einstein and Fermi-Dirac distributions, respectively.

At zero temperature ( $T = 0$ ,  $\beta \rightarrow \infty$ ,  $\mu \rightarrow \mu_0$ ) the parameters  $\xi_j$  reduce to

$$\begin{aligned} \varepsilon_j > \mu_0 & : \quad \xi_j = e^{\beta(\varepsilon_j - \mu_0)} \rightarrow \infty \quad \Rightarrow \quad \omega(\xi_j) \rightarrow \infty \quad , \\ \varepsilon_j < \mu_0 & : \quad \xi_j = e^{\beta(\varepsilon_j - \mu_0)} \rightarrow 0 \quad \Rightarrow \quad \omega(\xi_j) \rightarrow 0 \end{aligned} \quad (2.55)$$

and hence

$$\bar{n}_j = \begin{cases} 0 & , \quad \varepsilon_j > \mu_0 \\ \frac{1}{g} & , \quad \varepsilon_j < \mu_0 . \end{cases} \quad (2.56)$$

We can see that particles obeying the fractional exclusion statistics exhibit a Fermi surface under which  $\frac{1}{g}$  particles on average occupy one quantum state.

Now, the obvious question is whether the particles obeying the fractional exclusion statistics are indeed the anyons that we defined in (2.20) through the nontrivial phase acquired upon an exchange of two particles. One can compare the thermodynamic properties

of an ideal gas of particles obeying the fractional exclusion statistics and a gas of particles interacting through the statistical interaction (2.26). In the latter case, the virial expansion is used. Although only the second virial coefficient is completely known and the third one is known only partially, the conclusion is that an ideal anyon gas is *not* an ideal gas of particles obeying the fractional exclusion statistics. There have been several other attempts to introduce the fractional statistics, but non of them agrees with the thermodynamics of anyons. See [3] for the analysis.

# Chapter 3

## Anyons in experiments

The concept of anyons, these somewhat exotically behaving particles, sounds quite attractive. Sooner or later, however, one should ask the question whether his new ambitious theory has anything to do with reality. Finding a physical implementation of the new ideas can provide even stronger motivation and encourage further research. In this chapter we will talk about two experiments relevant for the physics of anyons. Firstly and mainly, we will discuss the quantum Hall effect which is widely agreed on proving the existence of anyons in real physical systems. In the second part we will briefly review the role of anyons in the theory of high-temperature superconductivity. Although it has been suggested that anyons could provide a mechanism for this yet unexplained phenomenon, experimental results indicate that they are, unfortunately, not involved.

### 3.1 Quantum Hall effect

In this section we will overview some aspects of the monolayer quantum Hall effect (QHE).<sup>1</sup> The QHE is of two kinds — the *integer* QHE and the *fractional* QHE. Especially the fractional QHE is interesting for us, because it supports quasiparticles with anyonic statistics.

Suppose electrons are moving in the  $xy$  plane in a perpendicular magnetic field  $\mathbf{B} = (0, 0, -B)$ ,  $B > 0$ , and suppose their velocity is constant and pointing in the  $x$  direction,  $\mathbf{v} = (v_x, 0, 0)$ . The electrons feel the Lorentz force and their motion is described by the equation

$$M\dot{\mathbf{v}} = -e(\mathbf{E} + \mathbf{v} \times \mathbf{B}) , \quad (3.1)$$

---

<sup>1</sup>There are also other types of quantum Hall effects (bilayer QHE, QHE in graphene). See a monograph about quantum Hall effects and their aspects written by Z. F. Ezawa [16].

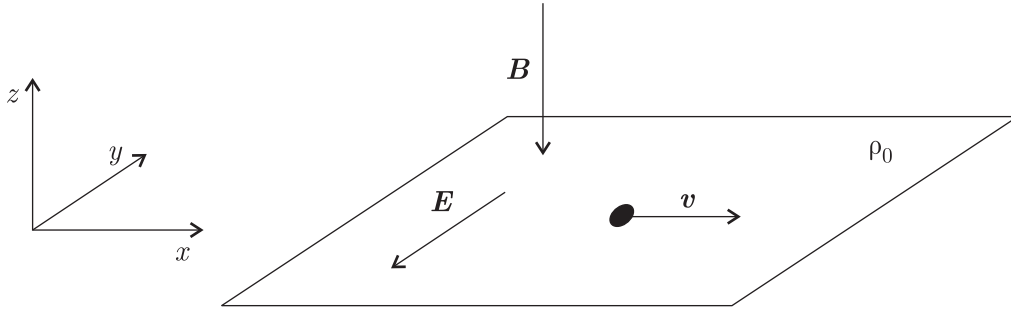


Figure 3.1: Electron gas of the density  $\rho_0$  is moving in the  $xy$  plane with a constant velocity  $\mathbf{v} = (v_x, 0, 0)$ . Perpendicular magnetic field  $\mathbf{B} = (0, 0, -B)$ ,  $B > 0$ , generates the Lorentz force that is compensated by the electric field  $\mathbf{E} = (0, E_y, 0) = (0, -v_x B, 0)$ .

where  $M$  is the mass of an electron and  $-e$  is its charge. The requirement of constancy of the velocity  $\mathbf{v}$  determines the electric field

$$\mathbf{E} = -\mathbf{v} \times \mathbf{B} \quad , \quad \text{i.e.} \quad E_x = 0 \quad \text{and} \quad E_y = -v_x B \quad . \quad (3.2)$$

In a homogeneous electron gas with the areal density  $\rho_0$  the current density is  $\mathbf{j} = -e\rho_0\mathbf{v}$ , hence we have the relation

$$j_x = \frac{e\rho_0}{B} E_y \quad . \quad (3.3)$$

The ratio between  $E_y$  and  $j_x$  is the *Hall resistivity*

$$R_{xy} \equiv \frac{E_y}{j_x} = \frac{B}{e\rho_0} = \frac{1}{\nu} \frac{2\pi\hbar}{e^2} \quad , \quad (3.4)$$

where  $\nu = \frac{2\pi\hbar\rho_0}{eB}$  is called the *filling factor* for reasons that will be settled later.

While classically, at a fixed density  $\rho_0$ , the Hall resistivity  $R_{xy}$  is a linear function of the perpendicular magnetic field strength  $B$ , experimentally, at low temperatures and high  $B$ , one finds that  $R_{xy}$  develops a series of plateaux (illustrated schematically in Fig.3.2), where it is constant around particular "magic" values of the filling factors  $\nu$ . This is known as the quantum Hall effect. The integer QHE (at  $\nu = \text{integer}$ ) was discovered by Klitzing [17] in 1980, a century after the discovery of Edwin Hall [18]. The fractional QHE (at  $\nu = n/m$  with integer  $n$  and odd integer  $m$ ) was discovered by Tsui, Störmer and Gossard [19] in 1982.

### 3.1.1 Electron gas confined to two dimensions

We consider a system where electrons are trapped in a thin layer ( $\sim 10\text{nm}$ ) between a semiconductor and an insulator or between two semiconductors. The electrons are free

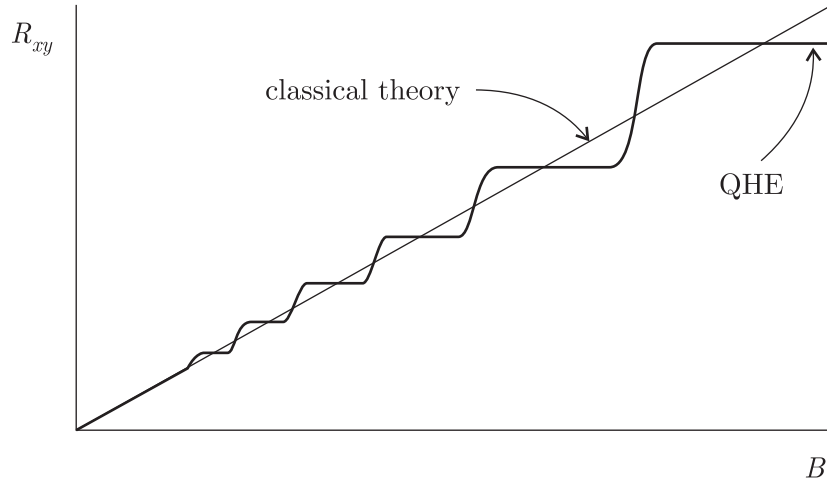


Figure 3.2: QHE is illustrated schematically. At a fixed density  $\rho_0$  of the electron gas, the classical theory predicts a linear dependence of the Hall resistivity  $R_{xy}$  on the magnetic field strength  $B$  (the thin line). Experimental results at low temperatures and strong magnetic fields, however, form a series of plateaux (the thick line). The values of  $R_{xy}$ , where the plateaux occur, are universal — they don't depend on properties of the sample.

to move in the  $x$  and  $y$  direction. The trap in the  $z$  direction is realized by a narrow potential well  $V(z)$  and with a help of sufficiently low temperature. It is then a good approximation that the electrons are confined to the ground state of the potential well and the 3-dimensional system is reduced to the 2-dimensional one. The wave function of one electron is of the form

$$\psi(x, y, z) = \psi(\mathbf{x})\psi_0(z) , \quad (3.5)$$

where  $\mathbf{x} = (x, y)$ . One only has to deal with the wave function  $\psi(\mathbf{x})$  of the planar system, since  $\psi_0(z)$  is the fixed ground state of the potential well.

It is instructive to approximate  $V(z)$  by the  $\delta$ -function potential:  $V(z) = -V_0\delta(z)$ ,  $V_0 > 0$ . The one dimensional Schrödinger equation is easily solved and the only bound state is given by

$$\psi_0(z) = \sqrt{\beta}e^{-\beta|z|} , \quad E_0 = -\frac{\hbar^2\beta^2}{2M} , \quad (3.6)$$

where  $\beta = \frac{MV_0}{\hbar^2}$  and  $M$  is the electron mass. For sufficiently deep potential well ( $\beta \rightarrow \infty$ ) the particle is confined at  $z = 0$ .

If we decide to model the well as infinitely deep but of a finite width  $L$ , the bound state energies are

$$E_n = \frac{\hbar^2\pi^2(n+1)^2}{2ML^2} , \quad n \geq 0 . \quad (3.7)$$

Since the energy gap  $E_1 - E_0 = \frac{3\hbar^2\pi^2}{2ME^2}$  increases as the width  $L \rightarrow 0$ , the electrons are well confined to the ground state for small  $L$  and sufficiently low temperatures.

The Coulomb interaction between electrons in three dimensions is given by

$$H_C = \frac{1}{2} \int d^3x d^3x' \frac{\rho_e(\mathbf{x}, z) \rho_e(\mathbf{x}', z')}{4\pi\epsilon \sqrt{(\mathbf{x} - \mathbf{x}')^2 + (z - z')^2}}, \quad (3.8)$$

where  $\rho_e(\mathbf{x}, z)$  is the electric charge density. For planar electrons we approximate the charge density as

$$\rho_e(\mathbf{x}, z) = -e\delta(z)\rho(\mathbf{x}), \quad (3.9)$$

with the particle density  $\rho(\mathbf{x}) = \sum_{r=1}^N \delta^{(2)}(\mathbf{x} - \mathbf{x}_r)$ , where  $\mathbf{x}_1, \dots, \mathbf{x}_N$  denote the positions of the electrons in the plane. The Coulomb energy term then reads

$$H_C = \frac{e^2}{2} \int d^2x d^2x' \frac{\rho(\mathbf{x})\rho(\mathbf{x}')}{4\pi\epsilon|\mathbf{x} - \mathbf{x}'|}. \quad (3.10)$$

The total Hamiltonian

$$H = H_C + H_K + H_Z \quad (3.11)$$

consists of the Coulomb term  $H_C$ ; the kinetic term

$$H_K = \frac{1}{2M} \sum_{r=1}^N (-i\hbar\nabla_r + e\mathbf{A}^{ext}(\mathbf{x}_r))^2, \quad (3.12)$$

where  $M$  is the electron mass and  $\mathbf{A}^{ext}(\mathbf{x})$  is the external electromagnetic potential; and the Zeeman term

$$H_Z = -\frac{\Delta_Z}{2} \int d^2x (\rho^\uparrow(\mathbf{x}) - \rho^\downarrow(\mathbf{x})), \quad (3.13)$$

where  $\Delta_Z \equiv |g\mu_B B|$  is the Zeeman gap,  $\rho^\uparrow(\mathbf{x})$  and  $\rho^\downarrow(\mathbf{x})$  are the number densities of up-spin and down-spin electrons.

To reveal the essence of the QH system, we will consider the *spin-frozen* theory, where the Zeeman gap is very large and all spins are frozen into their polarized states. The spin-full theory is discussed in [16]. It supports topological solitons called *skyrmions*, which are solutions to the corresponding nonlinear sigma model.

### 3.1.2 Planar electron in a magnetic field

For the time being, we will neglect the interaction due to the Coulomb term  $H_C$  to study the basic nature of planar electrons. The one electron Hamiltonian is given by

$$H = H_K = \frac{1}{2M} \left( (-i\hbar\partial_x + eA_x^{ext})^2 + (-i\hbar\partial_y + eA_y^{ext})^2 \right), \quad (3.14)$$

where the vector potential  $\mathbf{A}^{ext}(\mathbf{x})$  corresponds to the external magnetic field  $\mathbf{B} = (0, 0, -B)$ ,

$$0 < B = -\varepsilon_{jk}\partial_j A_k^{ext} = \partial_y A_x^{ext} - \partial_x A_y^{ext} . \quad (3.15)$$

The covariant momenta

$$\begin{aligned} P_x &\equiv -i\hbar\partial_x + eA_x^{ext} , \\ P_y &\equiv -i\hbar\partial_y + eA_y^{ext} \end{aligned} \quad (3.16)$$

and the newly defined *guiding center* coordinates

$$\begin{aligned} X &\equiv x + \frac{1}{eB}P_y , \\ Y &\equiv y - \frac{1}{eB}P_x \end{aligned} \quad (3.17)$$

satisfy the commutation relations

$$[X, P_x] = [X, P_y] = [Y, P_x] = [Y, P_y] = 0 . \quad (3.18)$$

This follow from the commutation relations

$$[X, Y] = -\frac{i\hbar}{eB} = -i\ell_B^2 , \quad [P_x, P_y] = i\hbar eB = i\frac{\hbar^2}{\ell_B^2} , \quad (3.19)$$

where we have introduced the *magnetic length*

$$\ell_B = \sqrt{\frac{\hbar}{eB}} , \quad (3.20)$$

which gives the fundamental scale to the QH system. The coordinate  $\mathbf{x} = (x, y)$  of an electron is decomposed as  $\mathbf{x} = \mathbf{X} + \mathbf{R}$  into the guiding center coordinate  $\mathbf{X} = (X, Y)$  and the relative coordinate

$$\mathbf{R} = (R_x, R_y) = \left( -\frac{1}{eB}P_y, \frac{1}{eB}P_x \right) . \quad (3.21)$$

The guiding center coordinate  $\mathbf{X}$  is constant in time as follows from the Heisenberg equations of motion (recall that  $H = \frac{1}{2M}(P_x^2 + P_y^2)$ )

$$\begin{aligned} \frac{dX}{dt} &= \frac{1}{i\hbar}[X, H] = 0 , \\ \frac{dY}{dt} &= \frac{1}{i\hbar}[Y, H] = 0 . \end{aligned} \quad (3.22)$$

The relative coordinate  $\mathbf{R}$  describes the motion around the guiding center. The corresponding Heisenberg equations

$$\begin{aligned}\frac{dR_x}{dt} &= \frac{1}{i\hbar}[R_x, H] = \frac{1}{i\hbar} \frac{1}{eB} \frac{1}{2M} [-P_y, P_x^2 + P_y^2] = \frac{1}{M} P_x = \frac{eB}{M} R_y, \\ \frac{dR_y}{dt} &= -\frac{eB}{M} R_x\end{aligned}\quad (3.23)$$

are most easily solved if we notice that they are equivalent to a single equation

$$\frac{d}{dt}(R_x + iR_y) = \omega_c R_y - i\omega_c R_x = -i\omega_c(R_x + iR_y), \quad (3.24)$$

where

$$\omega_c = \frac{eB}{M} = \frac{\hbar}{M\ell_B^2} \quad (3.25)$$

is the *cyclotron frequency*. We can integrate (3.24),

$$(R_x + iR_y)(t) = (R_x^0 + iR_y^0)e^{-i\omega_c t}, \quad (3.26)$$

i.e.

$$\begin{aligned}R_x(t) &= R_x^0 \cos \omega_c t + R_y^0 \sin \omega_c t, \\ R_y(t) &= R_y^0 \cos \omega_c t - R_x^0 \sin \omega_c t,\end{aligned}\quad (3.27)$$

where  $R_x^0$  and  $R_y^0$  are the integration constants. The relative coordinate  $\mathbf{R}$  makes cyclotron motion with the cyclotron frequency  $\omega_c$ .

It proves useful to introduce two pairs of operators

$$\begin{aligned}a &\equiv \frac{\ell_B}{\sqrt{2}\hbar}(P_x + iP_y), & a^\dagger &\equiv \frac{\ell_B}{\sqrt{2}\hbar}(P_x - iP_y) \\ b &\equiv \frac{1}{\sqrt{2}\ell_B}(X - iY), & b^\dagger &\equiv \frac{1}{\sqrt{2}\ell_B}(X + iY),\end{aligned}\quad (3.28)$$

obeying

$$\begin{aligned}[a, a^\dagger] &= [b, b^\dagger] = 1, \\ [a, b] &= [a^\dagger, b] = 0,\end{aligned}\quad (3.29)$$

which can be regarded as creation ( $a^\dagger$  and  $b^\dagger$ ) and annihilation ( $a$  and  $b$ ) operators of two independent harmonic oscillators. We may define the Fock vacuum  $|0\rangle$  by requiring

$$a|0\rangle = 0, \quad b|0\rangle = 0 \quad (3.30)$$

and construct the Fock states upon it,

$$|N, n\rangle = \sqrt{\frac{1}{N!n!}} (a^\dagger)^N (b^\dagger)^n |0\rangle . \quad (3.31)$$

In terms of the ladder operators  $a, a^\dagger$  the Hamiltonian (3.14) is rewritten as

$$\begin{aligned} H &= \frac{1}{2M}(P_x^2 + P_y^2) = \frac{1}{2M} \left( (P_x - iP_y)(P_x + iP_y) - i[P_x, P_y] \right) \\ &= \frac{1}{2M} \left( \frac{2\hbar^2}{\ell_B^2} a^\dagger a + \frac{\hbar^2}{\ell_B^2} \right) = \hbar\omega_c \left( a^\dagger a + \frac{1}{2} \right) . \end{aligned} \quad (3.32)$$

The energy levels, called the *Landau levels*, are found in the same way as for the harmonic oscillator:

$$E_N = \hbar\omega_c \left( N + \frac{1}{2} \right) \quad (3.33)$$

with the eigenstates  $|N, n\rangle$ ,<sup>2</sup> where  $n$  corresponds to the degeneracy within a Landau level. A state  $|N, n\rangle$  is called the *Landau site* and due to the Pauli exclusion principle it can accommodate one electron in the spin-less theory and two electrons in the theory with spins.

At this stage we choose the gauge, i.e. the electromagnetic potential  $\mathbf{A}^{ext}(\mathbf{x})$  such that  $B = \partial_y A_x^{ext} - \partial_x A_y^{ext}$ . We will work in the *symmetric gauge*

$$A_x^{ext} = \frac{1}{2}By \quad , \quad A_y^{ext} = -\frac{1}{2}Bx \quad , \quad (3.34)$$

in which the covariant momentum  $\mathbf{P}$  and the guiding center  $\mathbf{X}$  take the concrete form

$$\begin{aligned} P_x &= -i\hbar \frac{\partial}{\partial x} + \frac{eB}{2}y \quad , \quad P_y = -i\hbar \frac{\partial}{\partial y} - \frac{eB}{2}x \quad , \\ X &= \frac{1}{2}x - \frac{i\hbar}{eB} \frac{\partial}{\partial y} \quad , \quad Y = \frac{1}{2}y + \frac{i\hbar}{eB} \frac{\partial}{\partial x} . \end{aligned} \quad (3.35)$$

The angular momentum operator (there is only one in a two dimensional system) is given by

$$L \equiv -i\hbar x \frac{\partial}{\partial y} + i\hbar y \frac{\partial}{\partial x} = \frac{eB}{2}(X^2 + Y^2) - \frac{1}{2eB}(P_x^2 + P_y^2) = \hbar(b^\dagger b - a^\dagger a) . \quad (3.36)$$

The states  $|N, n\rangle$  are the eigenstates of  $L$ ,

$$L|N, n\rangle = \hbar(b^\dagger b - a^\dagger a)|N, n\rangle = \hbar(n - N)|N, n\rangle , \quad (3.37)$$

---

<sup>2</sup>The quantum numbers  $N$  and  $n$  correspond, respectively, to the ‘‘oscillators’’  $a$  and  $b$ .

with eigenvalues  $\hbar(n - N)$ . Thus,  $b$  and  $b^\dagger$ , respectively, are the operators decreasing and increasing the angular momentum of an electron.

We will now find the wave functions  $|N, n\rangle$  explicitly. It is convenient to introduce a pair of complex conjugate dimensionless coordinates

$$z = \frac{1}{2\ell_B}(x + iy) \quad , \quad z^* = \frac{1}{2\ell_B}(x - iy) \quad (3.38)$$

and the corresponding differential operators

$$\frac{\partial}{\partial z} = \ell_B \left( \frac{\partial}{\partial x} - i \frac{\partial}{\partial y} \right) \quad , \quad \frac{\partial}{\partial z^*} = \ell_B \left( \frac{\partial}{\partial x} + i \frac{\partial}{\partial y} \right) . \quad (3.39)$$

The ladder operators (3.28) now take the form

$$\begin{aligned} a &= -\frac{i}{\sqrt{2}} \left( z + \frac{\partial}{\partial z^*} \right) \quad , \quad a^\dagger = \frac{i}{\sqrt{2}} \left( z^* - \frac{\partial}{\partial z} \right) \quad , \\ b &= \frac{1}{\sqrt{2}} \left( z^* + \frac{\partial}{\partial z} \right) \quad , \quad b^\dagger = \frac{1}{\sqrt{2}} \left( z - \frac{\partial}{\partial z^*} \right) . \end{aligned} \quad (3.40)$$

In analogy with the harmonic oscillator, the states in the lowest Landau level ( $N = 0$ ) must satisfy

$$a|\psi\rangle = 0 \quad , \quad \text{i.e.} \quad -\frac{i}{\sqrt{2}} \left( z + \frac{\partial}{\partial z^*} \right) \psi(\mathbf{x}) = 0 \quad (3.41)$$

with the solution

$$\psi(\mathbf{x}) = \lambda(z)e^{-zz^*} \quad , \quad (3.42)$$

where  $\lambda(z)$  is an arbitrary analytic function. The state  $|N = 0, n = 0\rangle = |\psi_0\rangle$  has to satisfy, in addition, the condition

$$b|\psi_0\rangle = 0 \quad , \quad \text{i.e.} \quad \frac{1}{\sqrt{2}} \left( z^* + \frac{\partial}{\partial z} \right) \psi_0(\mathbf{x}) = 0 . \quad (3.43)$$

Since  $\psi_0(\mathbf{x}) = \lambda_0(z)e^{-zz^*}$ , the latter reduces to

$$\left( z^* + \frac{\partial}{\partial z} \right) (\lambda_0(z)e^{-zz^*}) = \frac{\partial \lambda_0(z)}{\partial z} e^{-zz^*} = 0 \quad \Rightarrow \quad \lambda_0(z) = \text{const} . \quad (3.44)$$

The normalization condition for  $|\psi_0\rangle$  dictates  $\lambda_0(z) = (2\pi\ell_B^2)^{-1/2}$ , so that

$$\psi_0(\mathbf{x}) = \frac{1}{\sqrt{2\pi\ell_B^2}} e^{-|z|^2} = \frac{1}{\sqrt{2\pi\ell_B^2}} \exp\left(-\frac{x^2 + y^2}{4\ell_B^2}\right) . \quad (3.45)$$

The states  $|\psi_n\rangle = |0, n\rangle$  from the lowest Landau level, but with higher angular momenta, are obtained by repeated application of the  $b^\dagger$  operator on the vacuum  $|\psi_0\rangle$  (see (3.31)) —

$$\psi_n(\mathbf{x}) = \sqrt{\frac{1}{2^n n!}} \left( z - \frac{\partial}{\partial z^*} \right)^n \psi_0(\mathbf{x}) = \sqrt{\frac{2^n}{n! 2\pi \ell_B^2}} z^n e^{-|z|^2} . \quad (3.46)$$

In higher Landau levels the calculations get more complicated, leading to Laguerre polynomials.

The probability that the electron in a state  $|\psi_n\rangle$  is found at radius  $r = 2\ell_B|z|$  is given by

$$|\psi_n(\mathbf{x})|^2 = \frac{2^n}{n! 2\pi \ell_B^2} |z|^{2n} e^{-2|z|^2} \propto r^{2n} \exp\left(-\frac{r^2}{2\ell_B^2}\right) , \quad (3.47)$$

which has a sharp maximum at  $r_n = \sqrt{2n}\ell_B$ . The area of a circle with radius  $r_n$  is  $2\pi n\ell_B^2$ . It accommodates  $n$  Landau site ( $n$  possible values of the angular momentum), i.e. the area of one Landau site is  $\Delta S = 2\pi\ell_B^2$ . This holds for any Landau level, not only for the lowest one.

For a sample of area  $S$  there are

$$\frac{S}{\Delta S} = \frac{S}{2\pi\ell_B^2} = \frac{e}{2\pi\hbar} SB \equiv \frac{SB}{\Phi_D} \quad (3.48)$$

states in each Landau level. The constant  $\Phi_D = \frac{2\pi\hbar}{e}$  is the *Dirac flux quantum*. We define the Landau level *filling factor*  $\nu$  as the ratio between the total number of electrons in the system and the number of states available in one Landau level:

$$\nu := \frac{\rho_0 S}{\frac{SB}{\Phi_D}} = \frac{\rho_0 \Phi_D}{B} , \quad (3.49)$$

$\rho_0$  is the electron density.

### 3.1.3 Many-particle states

It is straightforward to determine the ground state of the system at filling factor  $\nu = 1$ , i.e. when the lowest Landau level is completely filled. This is a particular case in the integer QHE. For the wave function  $\Psi(\mathbf{x}_1, \dots, \mathbf{x}_N)$  of  $N$  electrons, where the appropriate  $N$  depends on the size of the system as  $N = \rho_0 S = \frac{SB}{\Phi_D}$ , the Pauli exclusion principle implies that it is given by the *Slater determinant* constructed from the one particle wave

functions (3.46),

$$\begin{aligned}
\Psi(\mathbf{x}_1, \dots, \mathbf{x}_N) &= \frac{1}{\sqrt{N!}} \begin{vmatrix} \psi_0(\mathbf{x}_1) & \psi_1(\mathbf{x}_1) & \cdots & \psi_{N-1}(\mathbf{x}_1) \\ \psi_0(\mathbf{x}_2) & \psi_1(\mathbf{x}_2) & \cdots & \psi_{N-1}(\mathbf{x}_2) \\ \vdots & \vdots & \ddots & \vdots \\ \psi_0(\mathbf{x}_N) & \psi_1(\mathbf{x}_N) & \cdots & \psi_{N-1}(\mathbf{x}_N) \end{vmatrix} \\
&\propto \begin{vmatrix} 1 & z_1 & \cdots & z_1^{N-1} \\ 1 & z_2 & \cdots & z_2^{N-1} \\ \vdots & \vdots & \ddots & \vdots \\ 1 & z_N & \cdots & z_N^{N-1} \end{vmatrix} e^{-\sum_{j=1}^N |z_j|^2} \\
&= \left( \prod_{r<s} (z_r - z_s) \right) e^{-\sum_{j=1}^N |z_j|^2}, \tag{3.50}
\end{aligned}$$

where we have recognized the *Vandermonde determinant*.

In the case of fractional QHE, the Landau levels are not filled completely. The fractional QH system develops a new type of collective ground state driven by the Coulomb repulsion between the electrons that has been neglected so far, but now it becomes necessary to explain the fractional QHE. A trial wave function of the ground state at filling factor  $\nu = \frac{1}{m}$ ,  $m$  odd, was first proposed by Laughlin [20],

$$\Psi_m(\mathbf{x}_1, \dots, \mathbf{x}_N) = N_m \left( \prod_{r<s} (z_r - z_s)^m \right) e^{-\sum_{j=1}^N |z_j|^2}, \tag{3.51}$$

where  $N_m$  is the normalization factor.

Several properties of this wave function are to be pointed out. It is antisymmetric under the exchange of any two electron positions. Since the prefactor  $\prod_{r<s} (z_r - z_s)^m$  is purely analytic, all particles are in the lowest Landau level and since it is a polynomial in  $z_1, \dots, z_N$ ,  $\Psi_m$  is an eigenstate of the total angular momentum operator  $\hbar \sum_r b_r^\dagger b_r$ . The Coulomb repulsion among electrons is also contained in the prefactor, which has a zero of order  $m$  at the points of coincidence  $z_r = z_s$ . The Laughlin wave function (3.51) is the particular state, in which all electrons, having their own cyclotron motion, are repelled from each other as much as possible. It is not an exact ground state, but it has a very high overlap with numerical solutions for the QHE computed for various kinds of repulsive potentials [20].

### 3.1.4 Quasiparticles in the fractional QHE

Quasiparticles in the FQHE are stable vortex solitons<sup>3</sup> carrying fractional electric charges. We shall see that they obey anyonic statistics, i.e. they are anyons. A *quasihole* is created at the origin by transforming the polynomial part of the Laughlin wave function (3.51) as follows

$$\Psi_m^+ = N^+ \left( \prod_k z_k \prod_{r<s} (z_r - z_s)^m \right) e^{-\sum_{j=1}^N |z_j|^2}, \quad (3.52)$$

[16] and [21]. This amounts to increasing the angular momentum of each electron by 1 and pushing the electrons outwards from the vortex center. Similarly, a *quasielectron* is created at the origin when the angular momentum of each particle decreases by 1 (and electrons are pulled towards the vortex center),

$$\Psi_m^- = N^- \left( \prod_k \frac{\partial}{\partial z_k} \prod_{r<s} (z_r - z_s)^m \right) e^{-\sum_{j=1}^N |z_j|^2}. \quad (3.53)$$

The wave functions  $\Psi_m^+$  and  $\Psi_m^-$ , being the eigenstates of the Hamiltonian as well as  $\Psi_m$ , do not decay in time. The size of quasiparticles is of the order of  $\ell_B$  (the magnetic length (3.20)). Quasiholes are easier to analyze, but results analogous to those that will be derived hold for quasielectrons as well.

The electric charge of a quasihole can be calculated using the concept of the *Berry phase*<sup>4</sup> [4]. The wave function describing a quasihole located at position  $z_\alpha$  is obtained from (3.52) by the shift  $z_k \rightarrow z_k - z_\alpha$  in the polynomial part,

$$\Psi_m^{+z_\alpha} = N_\alpha^+ \left( \prod_k (z_k - z_\alpha) \right) \Psi_m. \quad (3.54)$$

---

<sup>3</sup>On the classical level, solitons are extended objects (classical field configurations) that are not deformable continuously into a classical vacuum without violating the energy finiteness condition. One says that solitons are *topologically stabilized*.

<sup>4</sup>In quantum mechanics, the initial-state and final-state vectors of a cyclic evolution are related by a phase factor  $e^{i\varphi_B}$  (so called *geometric* or *Berry phase*), which can have observable consequences [22].

The concept of Berry phase was first published by M. V. Berry in 1984 [23] in the context of adiabatic evolution of a cyclic quantum system. Barry Simon explained the Berry phase mathematically as an *anholonomy* in the parameter space [24]. Later on, Y. Aharonov and J. Anandan showed that if the evolution is cyclic in the projective Hilbert space, the anholonomy is not based on the assumption of adiabaticity [25]. Many further generalizations showed that the Berry phase is a pure artefact of the geometry of the projective Hilbert space and hence is independent of the actual Hamiltonian (as long as the curve in the projective Hilbert space is not changed).

Let us transport the quasihole adiabatically along a closed loop  $\Gamma$  so that  $z_\alpha$  becomes a time-dependent parameter. Since the time dependence of  $\Psi_m^{+z_\alpha}(t)$  comes solely from  $z_\alpha(t)$ , we find that

$$\frac{d}{dt}\Psi_m^{+z_\alpha}(t) = \sum_k \frac{d \ln(z_k - z_\alpha(t))}{dt} \Psi_m^{+z_\alpha}(t) . \quad (3.55)$$

The formula for calculating the Berry phase [25],

$$\varphi_B = i \int_{t_0}^{t_1} \langle \psi(t) | \frac{d}{dt} | \psi(t) \rangle dt , \quad (3.56)$$

takes the form

$$\varphi_B = i \int_{t_0}^{t_1} \langle \Psi_m^{+z_\alpha}(t) | \sum_k \frac{d \ln(z_k - z_\alpha(t))}{dt} | \Psi_m^{+z_\alpha}(t) \rangle dt , \quad (3.57)$$

where the integral over  $t$  is evaluated from the time  $t_0$ , when the quasihole begins its tour, to the final time  $t_1$  when it returns to its original position. We will assume that the loop  $\Gamma$  is traversed counterclockwise. (3.57) can be rewritten in terms of the electron density in the state  $\Psi_m^{+z_\alpha}(t)$ ,

$$\rho(z) = \langle \Psi_m^{+z_\alpha}(t) | \sum_k \delta^{(2)}(z - z_k) | \Psi_m^{+z_\alpha}(t) \rangle , \quad (3.58)$$

so that

$$\begin{aligned} \varphi_B &= i \int_{t_0}^{t_1} dt \int d^2z \frac{d \ln(z - z_\alpha(t))}{dt} \rho(z) \\ &= i \int d^2z \int_{t_0}^{t_1} dt \frac{dz_\alpha(t)}{dt} \frac{\rho(z)}{z_\alpha(t) - z} \\ &= i \int d^2z \oint_\Gamma dz_\alpha \frac{\rho(z)}{z_\alpha - z} . \end{aligned} \quad (3.59)$$

Under the reasonable assumption that the density  $\rho(z)$  is a regular function, only the points  $z$  inside  $\Gamma$  will give non-vanishing contour integral  $\oint_\Gamma \frac{1}{z_\alpha - z} dz_\alpha = 2\pi i$ . Thus

$$\varphi_B = i \int_{<\Gamma} d^2z \rho(z) 2\pi i = -2\pi N_\Gamma , \quad (3.60)$$

where the symbol  $\int_{<\Gamma} d^2z$  denotes the integral over the region inside  $\Gamma$ , and  $N_\Gamma$  is the number of electrons that are in there.

It can be shown [16] that the density of electrons in the state  $\Psi_m^{+z_\alpha}$  is uniform, i.e.  $N_\Gamma = \rho_0 S_\Gamma$ , where  $S_\Gamma$  is the area inside the loop  $\Gamma$ . Then  $N_\Gamma$  can be related, using (3.49), to the magnetic flux  $\Phi_\Gamma = -BS_\Gamma$  penetrating the area enclosed by  $\Gamma$ ,

$$N_\Gamma = \nu \frac{BS_\Gamma}{\Phi_D} = -\nu \frac{\Phi_\Gamma}{\Phi_D} . \quad (3.61)$$

If we identify the Berry phase with the Aharonov-Bohm phase  $\varphi_{AB} = e^{\frac{i}{\hbar}q\Phi_\Gamma}$  (footnote ??) that a particle of charge  $q$  acquires when it is moved along a closed loop encircling a flux  $\Phi_\Gamma$ , we can deduce the unknown charge  $q$ :

$$\varphi_B = 2\pi\nu\frac{\Phi_\Gamma}{\Phi_D} = \frac{q\Phi_\Gamma}{\hbar} = \varphi_{AB} \Rightarrow q = \frac{2\pi\hbar}{\Phi_D}\nu. \quad (3.62)$$

Since by definition  $\Phi_D = \frac{2\pi\hbar}{e}$  and, in our case, the filling factor  $\nu = \frac{1}{m}$ , we obtain a bit exotic result for the electric charge of a quasihole

$$e_{qh} = \frac{e}{m}, \quad (3.63)$$

where  $e$  is the elementary charge.

Analogously, one can derive [26] that the electric charge of a quasielectron is

$$e_{qe} = -\frac{e}{m}. \quad (3.64)$$

To find the exchange parameter  $\alpha$  (2.20) between two quasiholes we utilize the wave function

$$\Psi_m^{+z_\gamma, +z_\beta} = N_{\alpha\beta}^{++} \left( \prod_k (z_k - z_\gamma)(z_k - z_\beta) \right) \Psi_m \quad (3.65)$$

and calculate the Berry phase of an adiabatic process when the quasihole at  $z_\gamma(t)$  is moved along a closed loop  $\Gamma$ , while the quasihole at  $z_\beta$  is kept fixed. Along the same lines as when we calculated the charge of a quasihole we arrive to

$$\varphi_B = i \int_{t_0}^{t_1} \langle \Psi_m^{+z_\gamma, +z_\beta}(t) | \frac{d}{dt} | \Psi_m^{+z_\gamma, +z_\beta}(t) \rangle dt = -2\pi \int_{<\Gamma} d^2z \rho(z), \quad (3.66)$$

where  $\rho(z)$  is the electron density in the two-quasihole state,

$$\rho(z) = \langle \Psi_m^{+z_\gamma, +z_\beta}(t) | \sum_k \delta^{(2)}(z - z_k) | \Psi_m^{+z_\gamma, +z_\beta}(t) \rangle. \quad (3.67)$$

If  $z_\gamma$  does not encircle  $z_\beta$  during its motion then  $\varphi_B = -2\pi N_\Gamma$ . This corresponds to the situation when the two quasiholes are not exchanged. On the other hand, if  $z_\beta$  is located in the interior of  $\Gamma$ , the electron density inside  $\Gamma$  is no longer constant and the number of electrons has to be diminished by  $\frac{1}{m}$ . This yields the Berry phase

$$\varphi_B = -2\pi \left( N_\Gamma - \frac{1}{m} \right). \quad (3.68)$$

The extra phase  $\frac{2\pi}{m}$ , that accounts for one winding, i.e. two exchanges of the quasiholes, is identified with  $2\alpha$ , where  $\alpha$  is the anyonic exchange parameter. Therefore

$$\alpha = \frac{\pi}{m}. \quad (3.69)$$

We conclude that quasiholes in the fractional QHE at filling  $\nu = \frac{1}{m}$ ,  $m = 3, 5, \dots$ , are anyons with exchange phase  $e^{i\frac{\pi}{m}}$ .

### 3.1.5 Hall plateaux

So far we have studied the QH effect precisely at filling factor

$$\nu = \frac{\rho_0 \Phi_D}{B} = \frac{1}{m}. \quad (3.70)$$

When the magnetic field  $B$  is increased by  $\Delta B$ , the number of Landau sites (3.48) increases by  $\frac{S\Delta B}{\Phi_D}$ , i.e. the filling factor  $\nu$  decreases. Each Landau site thus created accommodates one quasihole. When  $B$  decreases by  $\Delta B$ , the number of Landau sites decreases by  $\frac{S\Delta B}{\Phi_D}$ ,  $\nu$  increases and for each missing Landau site a quasielectron is created.

Since both electrons and quasiparticles are electrically charged, the Hall current is carried by both of them and the Hall resistivity  $R_{xy}$  (3.4) is a linear function of  $B$ . But, this is only true in pure samples. Real samples contain impurities that localize the quasiparticles. In the vicinity of the magic filling factors  $\nu = \frac{1}{m}$ , only free electrons contribute to the Hall current, which leads to the formation of Hall plateaux around  $\nu = \frac{1}{m}$  (Fig.3.3). As the filling factor changes further, a Hall plateau is broken eventually since too many quasiparticles are created to be localized by impurities.

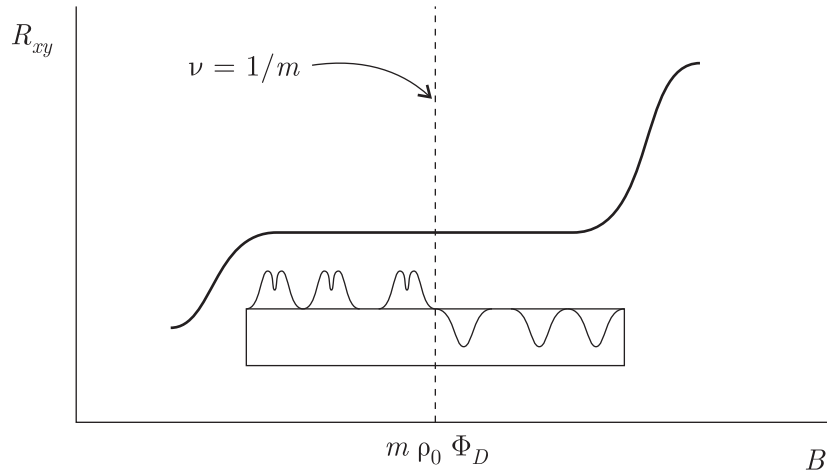


Figure 3.3: Quasielectrons are excited for  $B > m\rho_0\Phi_D$  and quasiholes are excited for  $B < m\rho_0\Phi_D$ . They are trapped by impurities and don't contribute to the Hall current. The Hall current remains unchanged in the vicinity of  $\nu = \frac{1}{m}$ , as is the origin on the Hall plateau.

## 3.2 High-temperature superconductivity

Anyons gained a lot of attention when it was realized that they could provide a mechanism for the high- $T_c$  superconductivity, observed in cuprate and other materials. The current picture is that a gas of *semions*, i.e. anyons with the exchange parameter  $\alpha = \frac{\pi}{2}$ , exhibits superfluidity and becomes superconducting if the anyons are electrically charged [27]. However, it is an open question whether this mechanism can be observed experimentally in nature.

As discussed in (2.27), anyons violate discrete symmetries of parity ( $P$ ) and time reversal ( $T$ ). Therefore, by experience, their presence in a material should cause optical effects. For example, linearly polarized light passing through sugar water rotates its direction of polarization due to a definite handedness of the molecules in the solution. Another example which breaks both ( $P$ ) and ( $T$ ) symmetries is the *Faraday effect*. In this effect, the direction of polarization of a linearly polarized light is rotated due to a magnetic field applied to the sample in the direction of propagation. When the light is reflected and travels back through the sample in the opposite direction, it does not “unrotate” its polarization axis into the original state but rather rotates once again in the same direction (time reversal violation).

It was suggested that the presence of anyons in the high- $T_c$  materials should cause effects similar to the Faraday effect. However, a careful experiment by Spielman *et al.* [28] has found no signal of time reversal violation. It seems that anyons do not provide a mechanism for the high- $T_c$  superconductivity in the observed compounds (see [3], chapter 9 for more details). On the other hand, this does not rule out the possibility that anyonic superconductors exist, but are yet to be discovered.

# Chapter 4

## Propagation of anyons on the toric code

In quantum information theory, the toric code is a model that can serve as a platform for quantum computational tasks. In particular, it can serve as a quantum memory — a device that stores quantum information. The lifetime of such memory is the central issue that decides about its potential practical usefulness. Excited states of the toric code are interpreted as anyons. Under perturbations, these anyons can propagate and cause logical errors. Our goal is to investigate the time evolution of the anyons living on the toric code and to see whether a disorder imprinted in the system can guarantee their (Anderson) localization.

### 4.1 Toric code — introduction

Quantum computer is a very powerful device. It can solve certain computational problems qualitatively faster than an ordinary computer. For example, there is no published classical algorithm decomposing efficiently an integer into its prime factors, yet a quantum algorithm running on a quantum computer has been proposed by Peter Shor [29], which resolves this problem in a time polynomial in the length of the input. Although there exist many quantum algorithms that push the frontiers of what computers can manage to resolve, the biggest challenge is the actual physical realization of a scalable and reliable quantum computer. This is because real quantum systems are vulnerable to interaction with the environment which causes decoherence of the quantum states, affects quantum information and consequently discredits the outcome of the computation. Shor's discovery of fault-tolerant quantum computation [30] allowed the building blocks of a quantum circuit, the

quantum gates, to be imperfect, that is to be close to the ideal ones up to a constant precision  $\delta$ . Unfortunately, the threshold value of  $\delta$  is very small (estimates vary) and thus hard to achieve.

Classical gates are, in contrast, reliable enough, therefore classical computation doesn't need to be performed fault-tolerantly. Consider, for example, how classical information is stored on a magnetic tape. Magnetism arises from spins of the individual atoms, each of which is quite sensitive to thermal fluctuations. The spins tend to be oriented in the same direction (to minimize the energy). If one spin is flipped to the opposite direction, its interaction with the other spins forces it to flip back — errors are being corrected at the physical level. In the quantum computational framework we can similarly propose a quantum code with local stabilizer operators. Such code was invented by Alexei Kitaev in 1997 [5].

Consider an  $N \times N$  square lattice with “torus-like” identification (Fig.4.1). There are

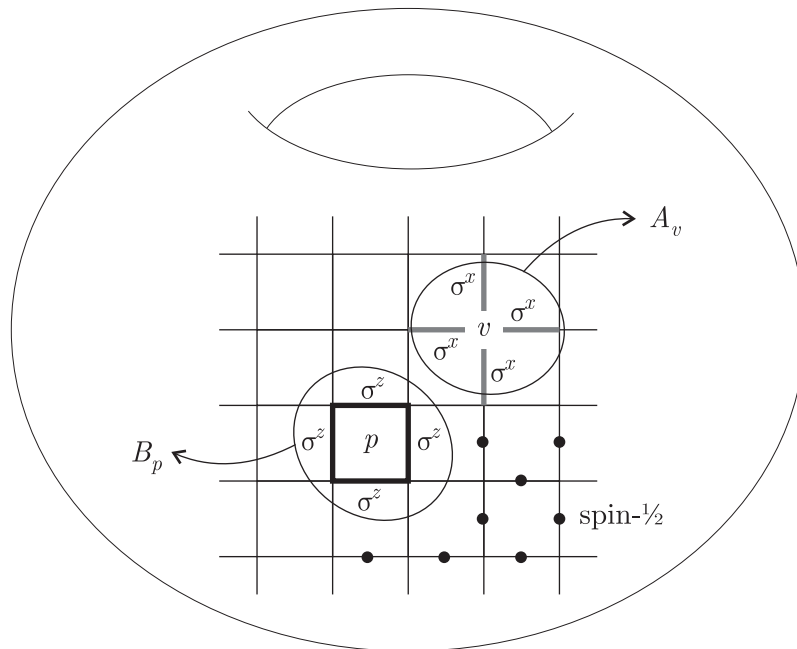


Figure 4.1: Toric code is a square lattice wrapped around a torus. Spin- $\frac{1}{2}$  particles are situated on each edge of the lattice and the stabilizer operators  $A_v$  and  $B_p$  are defined, respectively, for each vertex  $v$  and each plaquette  $p$ .

spin- $\frac{1}{2}$  particles located on each edge of the lattice. The total Hilbert space of this system is

$$\mathcal{H} = \mathcal{H}_2^{\otimes 2N^2} , \tag{4.1}$$

where  $\mathcal{H}_2$  is the Hilbert space of dimension 2 (one qubit space). So called *stabilizer operators* are defined around each vertex  $v$  and around each plaquette  $p$  of the lattice as follows:

$$A_v := \prod_{j \in \text{star}(v)} \sigma_j^x \quad B_p := \prod_{j \in \text{boun}(p)} \sigma_j^z, \quad (4.2)$$

with

$$\sigma_j^{x/z} = \bigotimes_{i \in \text{edges}} \begin{pmatrix} \sigma^{x/z} & \text{if } i = j \\ \mathbb{1} & \text{if } i \neq j \end{pmatrix}, \quad (4.3)$$

where  $\sigma^x$  and  $\sigma^z$  are the Pauli operators. The notation “ $j \in \text{star}(v)$ ” means that we take all (four) edges that connect to the vertex  $v$ . Similarly, “ $j \in \text{boun}(p)$ ” denotes the edges on the boundary of the plaquette  $p$ . Note that all  $A_v$ ’s and  $B_p$ ’s commute with each other because  $\text{star}(v)$  and  $\text{boun}(p)$  have either 0 or 2 common edges.<sup>1</sup> Also, they are Hermitian and have eigenvalues 1 and  $-1$ . There are all together  $2N^2$  stabilizers  $A_v, B_p$ .

Define the *protected subspace*  $\mathcal{L} \subseteq \mathcal{H}$  as

$$\mathcal{L} := \{|\xi\rangle \in \mathcal{H} \mid A_v|\xi\rangle = |\xi\rangle, B_p|\xi\rangle = |\xi\rangle \text{ for all } v, p\}. \quad (4.4)$$

Vectors in this subspace are supposed to represent quantum information. How much quantum information can we store? This is a question about the dimensionality of the subspace  $\mathcal{L}$ . We can observe that there are two relations between the stabilizer operators —

$$\prod_v A_v = \mathbb{1} \quad \prod_p B_p = \mathbb{1}, \quad (4.5)$$

so there are only  $2N^2 - 2$  independent stabilizers. Now, the handwaving argument is that since each (independent) condition in the definition of  $\mathcal{L}$  (4.4) halves the protected subspace, the dimension of  $\mathcal{L}$  is  $\frac{2^{2N^2}}{2^{2N^2-2}} = 4$ . A rigorous proof follows from the general theory of additive quantum codes [31, 32], but we will not discuss it here.

We will proceed similarly to the original Kitaev’s paper [5]. Consider paths  $c$  on the lattice, i.e. sequences  $c = (j_1, \dots, j_k)$ ,  $k \in \mathbb{N}$  of edges  $j_1, \dots, j_k$ , and similarly cuts  $c'$  of the lattice, i.e. paths on the dual lattice.<sup>2</sup> Some examples of these paths and cuts are depicted in Fig.4.2. To each path  $c$  we assign an operator  $Z_c$  by the prescription

$$c = (j_1, \dots, j_k) \mapsto Z_c := \prod_{i=1}^k \sigma_{j_i}^z \quad (4.6)$$

<sup>1</sup>For  $j \neq k$ :  $(\sigma_j^x \sigma_k^x)(\sigma_j^z \sigma_k^z) = -\sigma_j^z \sigma_j^x \sigma_k^x \sigma_k^z = (\sigma_j^z \sigma_k^z)(\sigma_j^x \sigma_k^x)$ .

<sup>2</sup>The dual lattice is defined (in the way usual in the graph theory) by declaring plaquettes of the original lattice vertices of the dual lattice and connecting all pairs of neighboring plaquettes of the original lattice by edges of the dual lattice. In our case, the dual lattice is the original one shifted in both directions by half the lattice spacing.

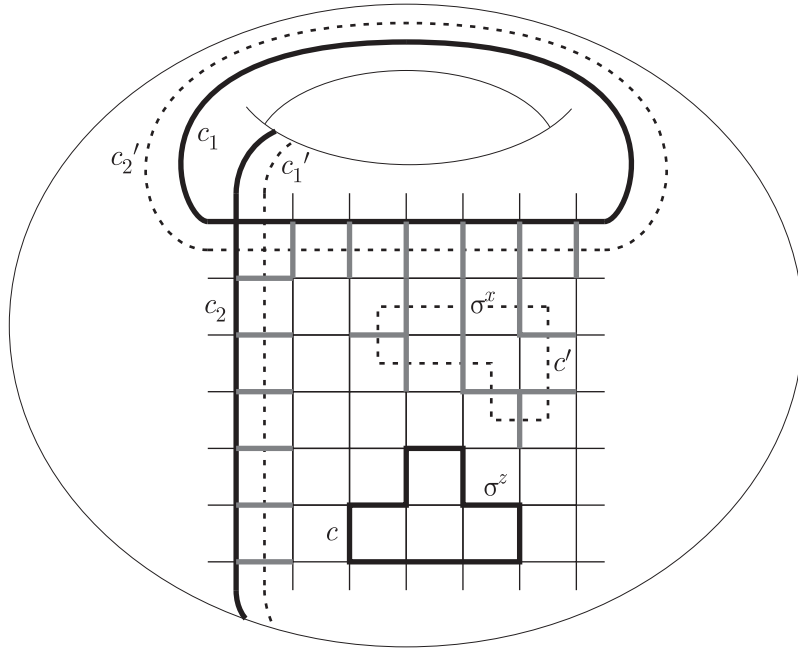


Figure 4.2: A generic path  $c$  on the lattice represents the operator  $Z_c$ . Two topologically nontrivial closed paths  $c_1$  and  $c_2$  define the operators  $Z_1$  and  $Z_2$  that act nontrivially on the protected subspace  $\mathcal{L}$ . Analogously, cuts  $c'$  of the lattice, i.e. paths on the dual lattice, represent the operators  $X_{c'}$ . Two topologically nontrivial closed cuts  $c'_1$  and  $c'_2$  are shown that define the operators  $X_1$  and  $X_2$ . These operators act nontrivially on  $\mathcal{L}$ .

and similarly to each cut  $c'$  we assign  $X_{c'}$  through

$$c' = (j'_1, \dots, j'_{k'}) \mapsto X_{c'} := \prod_{i=1}^{k'} \sigma_{j'_i}^x. \quad (4.7)$$

We observe that if  $c$  ( $c'$ ) is a closed loop then  $Z_c$  ( $X_{c'}$ ) commutes with all the stabilizers  $A_v$ ,  $B_p$  and therefore is a mapping from  $\mathcal{L}$  to  $\mathcal{L}$ . We also observe that if a loop  $c$  is contractible, i.e. if it is a boundary of some set of plaquettes  $P$ , the corresponding operator  $Z_c$  acts on  $\mathcal{L}$  as the identity operator,  $Z_c|\xi\rangle = |\xi\rangle$  for all  $|\xi\rangle \in \mathcal{L}$ , for it is a product of the stabilizers  $B_p$ ,  $p \in P$ . Similarly for the cuts  $c'$ . Thus, with respect to the protected subspace  $\mathcal{L}$ , only non-contractible loops and cuts are interesting.

On a torus we have two non-contractible loops (modulo the loops that are boundaries of some region) — the first homology group has two generators. We denote these loops  $c_1$  and  $c_2$  and the corresponding operators  $Z_1$  and  $Z_2$ . Analogously, two non-contractible cuts  $c'_1$  and  $c'_2$  define operators  $X_1$  and  $X_2$ . The loops  $c_1$ ,  $c_2$  and the cuts  $c'_1$ ,  $c'_2$  are drawn at Fig.4.2.

Realize that traveling any of these non-contractible loops or cuts twice yields the identity operator so going to higher winding numbers is fruitless. The 4 operators  $Z_1, Z_2, X_1, X_2$  have the same commutation relations as the operators  $(\sigma^z \otimes \mathbf{1}), (\mathbf{1} \otimes \sigma^z), (\sigma^x \otimes \mathbf{1}), (\mathbf{1} \otimes \sigma^x)$ . This is in agreement with the protected subspace being 4-dimensional, i.e.  $|\xi\rangle \in \mathcal{L}$  corresponding to a state of 2 qubits. The ground state of the toric code can encode 2 qubits of quantum information. Hence, we may hope to use the toric code as quantum memory.

## 4.2 Toric code Hamiltonian and anyonic excitations

Consider the Hamiltonian

$$H_0 = - \sum_{v \in \text{vertices}} A_v - \sum_{p \in \text{plaquettes}} B_p . \quad (4.8)$$

This Hamiltonian is more or less realistic, because it only involves local interactions — each stabilizer acts only on four nearby spin- $\frac{1}{2}$  particles. It is easy to diagonalize as all of the terms  $A_v, B_p$  commute. The ground state subspace coincides with  $\mathcal{L}$ ; it is 4-fold degenerate. Excited states occur if some of the constraints

$$A_v |\xi\rangle = |\xi\rangle \quad B_p |\xi\rangle = |\xi\rangle \quad (4.9)$$

are violated. Since the eigenvalues of  $A_v$  and  $B_p$  are  $\pm 1$ , the energy gap between the ground state and any of the excited states is  $\Delta E \geq 2$ .

Let us construct an excited state by taking a string (a connected path)  $t$ , as pictured in Fig.4.3(a), and applying the corresponding operator  $Z_t$  (recall the definition (4.6)) to some ground state  $|\xi\rangle$ . We obtain a state  $Z_t |\xi\rangle$  for which

$$A_{v_1} Z_t |\xi\rangle = -Z_t |\xi\rangle \quad \text{and} \quad A_{v_2} Z_t |\xi\rangle = -Z_t |\xi\rangle , \quad (4.10)$$

where  $v_1$  and  $v_2$  are the two distinct endpoints of an open string  $t$ . We interpret this violation the constraints (4.9) as two  $e$ -type particles occupying the vertices  $v_1, v_2$ . If  $t$  is a closed string then  $Z_t |\xi\rangle \in \mathcal{L}$  and no particles are created. Also note that for two strings  $t_1, t_2$  with common starting and ending points,  $Z_{t_1} |\xi\rangle = Z_{t_2} |\xi\rangle$  unless the loop “ $t_1$  followed by  $t_2$ ” winds around the torus.

Analogously, with a cut  $t'$  we have associated an operator  $X_{t'}$  (definition (4.7)). If  $t'$  has distinct endpoints  $p_1, p_2$  (see Fig.4.3(a)) then

$$B_{p_1} X_{t'} |\xi\rangle = -X_{t'} |\xi\rangle \quad \text{and} \quad B_{p_2} X_{t'} |\xi\rangle = -X_{t'} |\xi\rangle , \quad (4.11)$$

and we talk about two  $m$ -type particles occupying the plaquettes  $p_1$  and  $p_2$ .

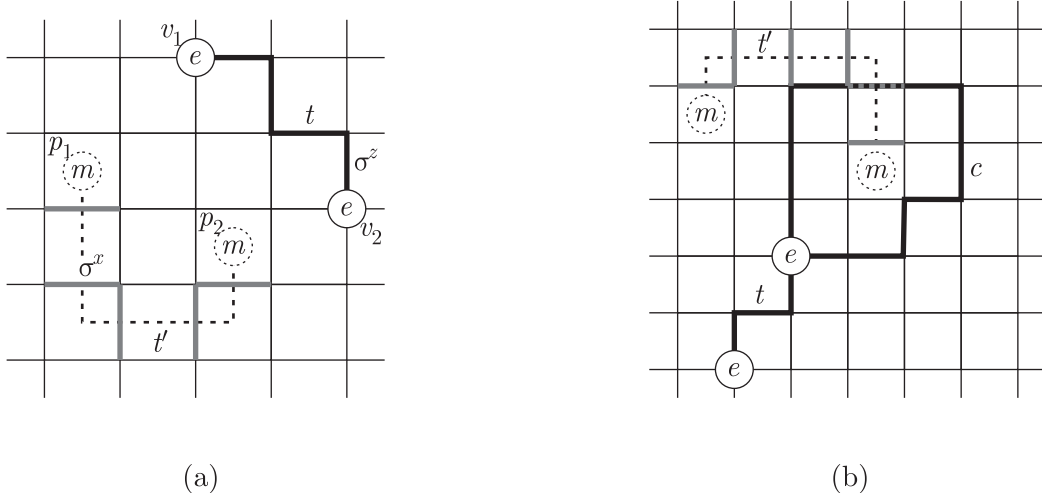


Figure 4.3: (a) A string  $t$  on the lattice represents the operator  $Z_t$ . The endpoints of  $t$  (vertices  $v_1$  and  $v_2$ ) are occupied by  $e$ -type particles. A string  $t'$  on the dual lattice represents the operator  $X_{t'}$ . The endpoints of  $t'$  (plaquettes  $p_1$  and  $p_2$ ) are occupied by  $m$ -type particles. (b) The initial configuration described by the strings  $t$  and  $t'$  presents a pair of  $e$  particles and a pair of  $m$  particles. If one of the  $e$  particles moves around one of the  $m$  particles (the cycle  $c$ ), the global wave function acquires a phase factor  $-1$ . This reveals anyonic statistics between the  $e$  and  $m$ -type particles.

### 4.2.1 Stability of a quantum memory

Suppose we initiate the toric code in a state  $|\xi\rangle \in \mathcal{L}$ . By doing so we have stored quantum information. The question is: What will be the state of the system after some time? Will it be  $|\xi\rangle$  or will it change? How reliable is our quantum memory?

Errors might occur characterized by an operator

$$E = \prod_{j \in \text{edges}} (\sigma_j^x)^{\alpha_j} \prod_{j \in \text{edges}} (\sigma_j^z)^{\beta_j}, \quad \alpha_j, \beta_j \in \{0, 1\} \quad (4.12)$$

acting on the initial state  $|\xi\rangle$ . The new state  $E|\xi\rangle$  is in general an excited state of the Hamiltonian  $H_0$ . It describes some configuration of  $e$  and  $m$ -type particles. The particles represent elementary errors, violations of the stabilizer conditions (4.9). They always come in pairs because of the relations (4.5).<sup>3</sup> Due to the energy gap  $\Delta E \geq 2$  between the ground state and the excited levels, which remains finite in the thermodynamic limit, errors are suppressed by coupling the toric code to a thermal bath with low temperature.

<sup>3</sup>Let, for instance,  $e$  particles be created at vertices from the set  $V_e = \{v \mid A_v E|\xi\rangle = -E|\xi\rangle\}$ . It holds

If the particles have been created, we can, in principle, bring them pairwise together to perform error correction. This is realized by a correction operator  $C$  acting upon  $E|\xi\rangle$  in such a way that the operator  $CE$  contains only closed strings, so that the resulting state  $CE|\xi\rangle$  lies in the protected subspace  $\mathcal{L}$ . If the error rate is below a certain threshold,<sup>4</sup> the error correction can be done through a minimum distance matching of the particle pairs without forming topologically nontrivial loops. The resulting state  $CE|\xi\rangle$  will be equal to the initial state  $|\xi\rangle$ , i.e. the quantum information will remain unchanged. If, however, the error rate is too high, we can't avoid creating topologically nontrivial loops (such as the operators  $Z_1, Z_2, X_1, X_2$ ). The state  $CE|\xi\rangle$  might then be different from  $|\xi\rangle$ , which results in a logical error — the information stored in the quantum memory is changed.

## 4.2.2 Anyonic statistics revealed

Consider a perturbation to the toric code Hamiltonian  $H_0$  (definition 4.8) of the form

$$V = -h_x \sum_{j \in \text{edges}} \sigma_j^x - h_z \sum_{j \in \text{edges}} \sigma_j^z, \quad (4.13)$$

where the constants  $h_x$  and  $h_z$  measure the strength of the perturbation. This perturbation does not commute with the original Hamiltonian  $H_0$ . The eigenstates of  $H_0$  are therefore no longer eigenstates of the perturbed Hamiltonian  $H = H_0 + V$ . As a consequence,  $e$  and  $m$  particles will propagate rather than stay at their initial positions.

What happens if the particles move around each other? Consider the initial state

$$|\Psi_i\rangle = X_{t'} Z_t |\xi\rangle, \quad |\xi\rangle \in \mathcal{L} \quad (4.14)$$

pictured in Fig.4.3(b), which describes a configuration of two  $e$  particles and two  $m$  particles. Let, for example, one of the  $e$  particles move around one of the  $m$  particles and end up at its initial position. The state of the system is now described by the wave function

$$|\Psi_f\rangle = Z_c X_{t'} Z_t |\xi\rangle = -X_{t'} Z_t Z_c |\xi\rangle = -|\Psi_i\rangle, \quad (4.15)$$

---

that

$$E|\xi\rangle = \left( \prod_v A_v \right) E|\xi\rangle = \left( \prod_{v \in V_e} A_v \right) \left( \prod_{v \notin V_e} A_v \right) E|\xi\rangle = \left( \prod_{v \in V_e} A_v \right) E|\xi\rangle = (-1)^{|V_e|} E|\xi\rangle,$$

where  $|V_e|$  denotes the number of elements of the set  $V_e$ .

<sup>4</sup>If  $P$  denotes the probability of an individual  $\sigma^x$  error, the threshold is estimated as  $P \approx 0.11$  [33]. The same holds for  $\sigma^z$  errors.

because the operators  $X_{\nu'}$  and  $Z_c$  anti-commute. We can see that the global wave function acquires a phase factor  $-1$ . The  $e$  and  $m$ -type particles are quite different from bosons and fermions, which do not change sign in such a process. Indeed, they are (Abelian) anyons and we will call them  $e$  anyons and  $m$  anyons from now on. Notice that the anyonic statistics is revealed only between  $e$  and  $m$  particles, not between  $e$  (or  $m$ ) particles themselves. In terms of the Aharonov-Bohm effect interpretation (footnote 5) we can view the  $e$  anyons as electric charges and  $m$  anyons as magnetic fluxes with appropriate combination ( $charge$ )  $\times$  ( $flux$ )  $= \pi$  so that the Aharonov-Bohm phase  $e^{i(charge)\times(flux)}$  is equal to  $-1$ .

The effect of the perturbation (4.13), which would be caused by a spurious magnetic field in any physical realization of the toric code, is to create, annihilate and transport! anyons. If this acts unchecked, even a single pair of anyons can form a topologically nontrivial loop around the torus, thus causing a logical error (a final state  $|\xi_f\rangle \in \mathcal{L}$  that is different from the initial state  $|\xi_i\rangle \in \mathcal{L}$ ). Therefore, to know how stable our quantum memory is, we need to investigate the propagation of errors, i.e. the anyons, on the toric code lattice. If they exhibit some sort of localization (at least under certain assumptions), the toric code will get one step closer to become a reliable quantum memory.

### 4.2.3 Perturbation induced anyonic quantum walks

Let us first make clear that the unperturbed Hamiltonian  $H_0$  defined in (4.8) doesn't induce any motion of the anyonic excitations. Choose an orthonormal basis of  $\mathcal{L}$ :  $\mathcal{L} = \text{span}\{|\xi_{--}\rangle, |\xi_{-+}\rangle, |\xi_{+-}\rangle, |\xi_{++}\rangle\}$ , where

$$Z_1|\xi_{s_1s_2}\rangle = s_1|\xi_{s_1s_2}\rangle \quad , \quad Z_2|\xi_{s_1s_2}\rangle = s_2|\xi_{s_1s_2}\rangle \quad . \quad (4.16)$$

Take two arbitrary configurations of anyons described by two sets of strings — the operators  $Z_t^{(i)}X_{\nu'}^{(i)}$  and  $Z_t^{(f)}X_{\nu'}^{(f)}$  — acting on some ground state  $|\xi_{s_1s_2}\rangle \equiv |\xi\rangle$ . We observe that the two states  $|i\rangle = Z_t^{(i)}X_{\nu'}^{(i)}|\xi\rangle$  and  $|f\rangle = Z_t^{(f)}X_{\nu'}^{(f)}|\xi\rangle$  are orthogonal,  $\langle f|i\rangle = 0$ , if they correspond to two different configurations of anyons, since in that case  $|i\rangle$  and  $|f\rangle$  are two distinct eigenvectors of some Hermitian operator  $A_v$  or  $B_p$ . Also,  $\langle f|i\rangle = 0$  if  $|i\rangle$  and  $|f\rangle$  describe the same anyonic configuration, but distinct logical states. Therefore, the matrix elements

$$\langle f|H_0|i\rangle = - \sum_v \langle f|A_v|i\rangle - \sum_p \langle f|B_p|i\rangle = - \sum_v \pm \langle f|i\rangle - \sum_p \pm \langle f|i\rangle \quad (4.17)$$

can be nonzero only for  $|i\rangle, |f\rangle$  describing identical anyonic configurations and logical states, i.e.  $H_0$  is diagonal in the basis of anyonic configurations. The time evolution of a

state  $|i\rangle$  is then trivial, only multiplying  $|i\rangle$  by the phase factor  $e^{iE_i}$ , i.e. the anyons don't move around.

Introducing a perturbation  $V$  as in (4.13) makes the anyons walk. We put  $h_x = 0$  for simplicity and  $h_z \equiv h$  for brevity. Now, the Hamiltonian of the system

$$H = H_0 + V = - \sum_{v \in \text{vert}} A_v - \sum_{p \in \text{plaq}} B_p - h \sum_{j \in \text{edges}} \sigma_j^z \quad (4.18)$$

leaves the  $m$ -type anyons static since for any configuration  $|i\rangle$  and any plaquette  $p$

$$B_p|i\rangle = s_p|i\rangle, \quad s_p \in \{-, +\} \quad \Rightarrow \quad B_p(H|i\rangle) = HB_p|i\rangle = s_p(H|i\rangle). \quad (4.19)$$

On the other hand,  $H$  induces a nontrivial evolution of the  $e$  anyons — a *continuous-time quantum walk*. To see this, realize that  $H$  has nonzero off-diagonal matrix elements. Given two states  $|i\rangle = Z_t^{(i)} X_{t'}^{(i)} |\xi\rangle$  and  $|f\rangle = Z_t^{(f)} X_{t'}^{(f)} |\xi\rangle$  we observe that

$$\begin{aligned} \langle f|(-V)|i\rangle &= h \sum_{j \in \text{edges}} \langle \xi | X_{t'}^{(f)} Z_t^{(f)} \sigma_j^z Z_t^{(i)} X_{t'}^{(i)} |\xi\rangle = h \langle \xi | X_{t'}^{(f)} Z_t^{(f)} \sigma_j^z Z_t^{(i)} X_{t'}^{(i)} |\xi\rangle \\ &= \pm h \langle \xi | Z_t^{(f)} \sigma_j^z Z_t^{(i)} X_{t'}^{(f)} X_{t'}^{(i)} |\xi\rangle = \pm h \langle \xi | \xi\rangle = \pm h \end{aligned} \quad (4.20)$$

if for some edge  $j$ ,  $Z_t^{(f)} \sigma_j^z Z_t^{(i)}$  forms a system of closed loops only and  $X_{t'}^{(i)}$ ,  $X_{t'}^{(f)}$  correspond to identical configuration of the  $m$  anyons. To determine the  $\pm$  sign one needs to calculate how many times the Pauli operators  $\sigma^x$  and  $\sigma^z$  are transposed when going from  $X_{t'}^{(f)} Z_t^{(f)} \sigma_j^z Z_t^{(i)} X_{t'}^{(i)}$  to the expression  $Z_t^{(f)} \sigma_j^z Z_t^{(i)} X_{t'}^{(f)} X_{t'}^{(i)}$ . For this purpose we recall the discussion related to Fig.4.3(b). The  $\pm$  depends on how many  $m$  anyons in the  $X_{t'}^{(f)}$  configuration are enclosed by the loops  $Z_t^{(f)} \sigma_j^z Z_t^{(i)}$  with “+” corresponding to an even number and “−” to an odd number of anyons. The result only depends on the positions of the  $m$  anyons and not on the particular way they are connected by the strings  $X_{t'}^{(f)}$ .

Our goal is to investigate how the  $e$  anyons will propagate under the action of the evolution operator  $e^{-itH}$ , given some fixed (random) configuration of the  $m$  anyons. In this context we would like to mention the Wootton's and Pachos' paper [7] where the authors consider a perturbed toric code Hamiltonian

$$H_{TC} + H_h = - \sum_v J_v A_v - \sum_p J_p B_p - h \sum_j \sigma_j^z. \quad (4.21)$$

and analyze the propagation of the  $e$  anyons with no  $m$  anyons present in the system. They show that if  $J_v$ 's are not uniform but take random values on each vertex and  $h \ll J_v$ , the disorder in the system can successfully localize the anyons by placing an exponential

bound on the length of their propagation. Their arguments are based on the theory of *Anderson localization* (see the original Anderson's paper [6] or a recent overview [34]).

In our case the  $J_v$ 's are uniform and for our choice of units  $J_v = 1$ . The random property of our system is the  $m$  anyon configuration. Does this kind of randomness lead to a localization of the  $e$  anyons as in [7] or does it not? To make the analysis more tractable we will investigate a simplified topological model. Instead of a torus we will define our code on a strip with one periodic identification. The lattice will resemble a ladder and we will refer to it as the *ladder lattice*.

### 4.3 Ladder lattice model

In analogy with the toric code, we define a stabilizer code on a ladder-like lattice with one identification depicted in Figure 4.4. There are  $N$  vertices in the horizontal direction and

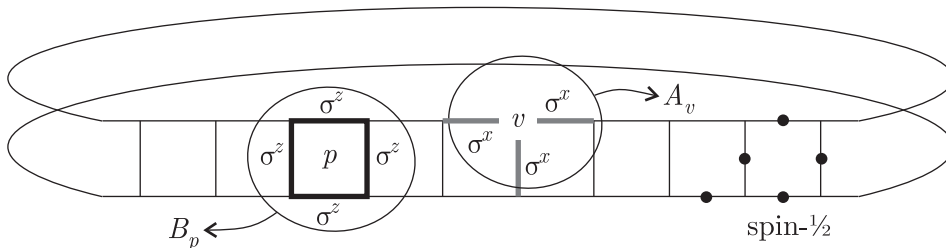


Figure 4.4: The stabilizer code defined on a square lattice on a strip — a ladder with one identification. Spin- $\frac{1}{2}$  particles are situated on each edge of the lattice and the stabilizer operators  $A_v$  and  $B_p$  are defined for each vertex  $v$  and plaquette  $p$ , respectively (in analogy with the original toric code, Fig.4.1).

2 vertices in the vertical direction. Spin- $\frac{1}{2}$  particles live on the edges of the lattice, the stabilizer operators  $A_v$  consist of three Pauli operators  $\sigma^x$  surrounding a vertex  $v$ ,

$$A_v := \prod_{j \in \text{star}(v)} \sigma_j^x, \quad (4.22)$$

and the stabilizer operators  $B_p$  form the boundary of a plaquette  $p$ ,

$$B_p := \prod_{j \in \text{boun}(p)} \sigma_j^z. \quad (4.23)$$

The protected subspace  $\mathcal{L} \subseteq \mathcal{H}$  contains vectors  $|\xi\rangle$  such that

$$A_v|\xi\rangle = |\xi\rangle, \quad B_p|\xi\rangle = |\xi\rangle \quad (4.24)$$

for all vertices  $v$  and plaquettes  $p$ . The subspace  $\mathcal{L}$  has dimension 2. Corresponding to this code is the unperturbed Hamiltonian

$$H_0 = - \sum_{v \in \text{vertices}} A_v - \sum_{p \in \text{plaquettes}} B_p, \quad (4.25)$$

the lowest energy eigenspace of which coincides with  $\mathcal{L}$ . An  $e$ -type anyon occurs on a vertex  $v$  whenever

$$A_v |\psi\rangle = -|\psi\rangle \quad (4.26)$$

and similarly an  $m$ -type anyon occurs on a plaquette  $p$  for which

$$B_p |\psi\rangle = -|\psi\rangle. \quad (4.27)$$

Anyons of both types are created in pairs and they occupy the endpoints of a string of  $\sigma^z$  operators (for the  $e$  anyons) and the endpoints of a cut of  $\sigma^x$  operators (for the  $m$  anyons).

We introduce a perturbation to  $H_0$  of the form  $V = -h \sum_j \sigma_j^z$ . The full Hamiltonian now reads

$$H = - \sum_{v \in \text{vertices}} A_v - \sum_{p \in \text{plaquettes}} B_p - h \sum_{j \in \text{edges}} \sigma_j^z \quad (4.28)$$

and it induces a quantum walk of the  $e$  anyons while keeping the  $m$  anyons static. The logical error occurs when one  $e$  anyon from a pair propagates all the way around the ladder and annihilates with its fellow  $e$  anyon. During this process a loop  $Z$  of  $\sigma^z$  matrices is formed which maps the logical state  $|\xi\rangle$  into another logical state  $Z|\xi\rangle$ , causing a logical error. Our goal is to probe how the  $e$  anyons will propagate in a static pattern of the  $m$  anyons. What effect will the nontrivial braiding properties of the anyons (recall Fig.4.3) have on their quantum walk?

We assume that the perturbation  $V$  is weak ( $h \ll 1$ ). Then the  $e$  anyon pairs are created sparsely and each pair can be considered independently. We will thus analyze a single pair only. Creation and annihilation of a pair of anyons is energetically suppressed by the energy gap  $\Delta E = 2$ .

Let us introduce some notation as suggested by Fig.4.5. We denote  $\mathcal{H}$  the Hilbert space of one  $e$  anyon configurations, i.e.

$$\mathcal{H} = \text{span}\{|x, y\rangle \equiv |x\rangle \otimes |y\rangle \mid x = 1, \dots, N, y = 0, 1\} \quad (4.29)$$

is the space of all positions (vertices) one  $e$  anyon can occupy. Let

$$M = \{m_1, \dots, m_{|M|}\} \subseteq \{1, \dots, N\} \quad (4.30)$$

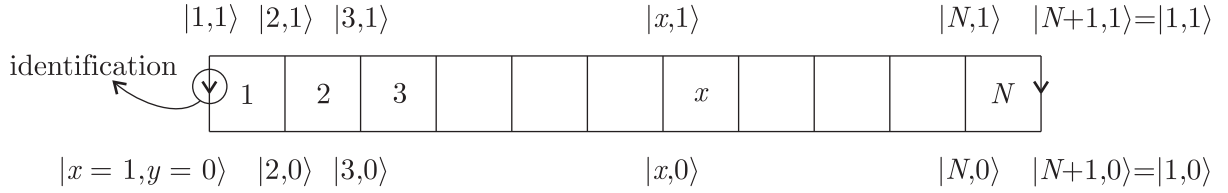


Figure 4.5: Vertices of the ladder are denoted by a pair  $x = 1, \dots, N$  (the horizontal axis) and  $y = 0, 1$  (the vertical axis). Each vertex corresponds to one basis vector of the one- $e$ -anyon Hilbert space  $\mathcal{H}$ . There are  $N$  plaquettes numbered by integers  $1, \dots, N$ . The identification on the two sides of the ladder is illustrated.

denote the set of plaquettes where  $m$  anyons are located. For a logical state  $|\xi\rangle \in \mathcal{L}$  we denote  $|\xi_M\rangle$  the state of  $|M|$  anyons of type  $m$  that have been created upon  $|\xi\rangle$  and moved to plaquettes from the set  $M = \{m_1, \dots, m_{|M|}\}$ .<sup>5</sup>

Once  $|\xi_M\rangle$  has been fixed and a pair of  $e$  anyons created we represent configurations of the two  $e$  anyons by the vectors  $|x_1, y_1\rangle \otimes |x_2, y_2\rangle \in \mathcal{H} \times \mathcal{H}$ .<sup>6</sup> To establish the connection with the original Hilbert space of the code (which is fully analogous to (4.1)) we need to choose a canonical manner in which the string  $Z_t$  connecting the two  $e$  anyons is laid down.<sup>7</sup> For this purpose choose and fix a point  $(x_0, 0)$  on the ladder. Let  $(x_1, y_1)$  and  $(x_2, y_2)$  be the positions of the two  $e$  anyons. The canonical string  $Z_{t_1}$  starts at  $(x_0, 0)$ , connects straightly and by the shortest way to the vertex  $(x_1, 0)$  and then to the vertex  $(x_1, y_1)$ . Accordingly,  $Z_{t_2}$  connects sequentially  $(x_0, 0)$ ,  $(x_2, 0)$  and  $(x_2, y_2)$ . The canonical string between the two positions  $(x_1, y_1)$  and  $(x_2, y_2)$  is the composition  $Z_t = Z_{t_1} Z_{t_2}$  (see Fig.4.6).

<sup>5</sup>More precisely,

$$|\xi_M\rangle = X_{t'} |\xi\rangle ,$$

where  $X_{t'}$  is a collection of strings of  $\sigma^x$  operators whose endpoints are  $m_1, \dots, m_{|M|}$ . The set  $M$  carries no information about a concrete layout of the strings. This information, however, is not important for the braiding properties of the anyons, which is what we want to probe. It is only important how many  $m$  anyons an  $e$  anyon encircles during its travel (see Fig.4.3 in this context).

<sup>6</sup>Strictly speaking, since the  $e$  anyons are indistinguishable, we should represent them by symmetrized vectors  $|x_1, y_1\rangle \otimes |x_2, y_2\rangle + |x_2, y_2\rangle \otimes |x_1, y_1\rangle$ . We will not be as punctual, because in a while we will reduce our problem to a one particle walk only.

<sup>7</sup>Keep in mind that  $Z_{t_1} |\xi_M\rangle$  and  $Z_{t_2} |\xi_M\rangle$  are the same quantum state (they differ only by a phase factor) if  $Z_c = Z_{t_1} Z_{t_2}$  is a closed contractible loop.

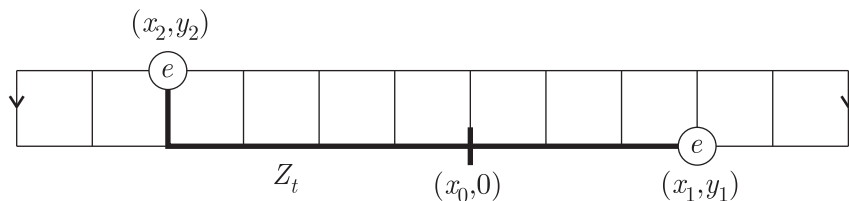


Figure 4.6: The definition of the canonical manner of connecting two  $e$  anyons by a string  $Z_t$ .

### 4.3.1 One anyon walk

The two  $e$  anyons are almost independent. The only correlation between them is the fact that their annihilation is energetically suppressed, so they cannot occupy the same position at the same time. We will neglect this correlation (in doing so we support the spreading slightly as we don't prohibit the steps that bring the two anyons to the same vertex) and analyze the propagation of one  $e$  anyon (the *walker*) only. For this purpose we fix the position of one of the anyons sufficiently far (say, on the horizontally opposite side of the ladder) from the other one, the walker.

We will induce the Hamiltonian  $H^I$ , a linear operator on the space of one anyon configurations  $\mathcal{H}$ , that describes the propagation of one  $e$  anyon in the presence of some fixed pattern of  $m$  anyons. Let us denote  $|\mathbf{x}\rangle \equiv |x, y\rangle \in \mathcal{H}$  and define

$$\langle \mathbf{x}_f | H^I | \mathbf{x}_i \rangle := \langle \xi_M | Z_t^{(f)} H Z_t^{(i)} | \xi_M \rangle, \quad (4.31)$$

where  $Z_t^{(i)}$  and  $Z_t^{(f)}$  are the canonical strings between the fixed anyon and the walker anyon at position  $\mathbf{x}_i$  and  $\mathbf{x}_f$ , respectively.  $H$  as defined in (4.28) consists of three sums — over vertices  $v$ , plaquettes  $p$  and edges  $j$ . We separate

$$H^I = H_v^I + H_p^I + H_e^I \quad (4.32)$$

and analyze the three parts one by one. From the discussion around the relation (4.17) it follows that

$$\begin{aligned} \langle \mathbf{x}_f | H_v^I | \mathbf{x}_i \rangle &= - \sum_v \langle \xi_M | Z_t^{(f)} A_v Z_t^{(i)} | \xi_M \rangle = - \left( \sum_{v \in \{\mathbf{x}_i, \bar{\mathbf{x}}\}} -1 + \sum_{v \notin \{\mathbf{x}_i, \bar{\mathbf{x}}\}} 1 \right) \delta_{\mathbf{x}_i, \mathbf{x}_f} \\ &= -(2N - 4) \delta_{\mathbf{x}_i, \mathbf{x}_f}, \end{aligned} \quad (4.33)$$

where  $2N$  is the number of vertices of the lattice,  $\bar{\mathbf{x}}$  is the position of the fixed  $e$  anyon

and  $\delta_{\mathbf{x}_i, \mathbf{x}_f} = 1$  if  $\mathbf{x}_i = \mathbf{x}_f$  and  $\delta_{\mathbf{x}_i, \mathbf{x}_f} = 0$  otherwise. Similarly,

$$\begin{aligned} \langle \mathbf{x}_f | H_p^I | \mathbf{x}_i \rangle &= - \sum_p \langle \xi_M | Z_t^{(f)} B_p Z_t^{(i)} | \xi_M \rangle = - \left( \sum_{p \in M} -1 + \sum_{p \notin M} 1 \right) \delta_{\mathbf{x}_i, \mathbf{x}_f} \\ &= -(N - 2|M|) \delta_{\mathbf{x}_i, \mathbf{x}_f} . \end{aligned} \quad (4.34)$$

The case of  $H_e$  is a bit more subtle, but it results from the relation (4.20) and the discussion that follows it:

$$\langle \mathbf{x}_f | H_e^I | \mathbf{x}_i \rangle = -h \sum_j \langle \xi_M | Z_t^{(f)} \sigma_j^z Z_t^{(i)} | \xi_M \rangle = -h \delta_{\langle \mathbf{x}_i, \mathbf{x}_f \rangle} s(\mathbf{x}_i, \mathbf{x}_f) , \quad (4.35)$$

where  $\delta_{\langle \mathbf{x}_i, \mathbf{x}_f \rangle} = 1$  if the vertex  $\mathbf{x}_i$  neighbors with  $\mathbf{x}_f$  and  $\delta_{\langle \mathbf{x}_i, \mathbf{x}_f \rangle} = 0$  otherwise. The factor  $s(\mathbf{x}_i, \mathbf{x}_f)$  accounts for the nontrivial braiding properties between  $e$  and  $m$ -type anyons:

$$s(\mathbf{x}_i, \mathbf{x}_f) = \begin{cases} -1 & \text{if } y_i = y_f = 1 \text{ and } \min(x_i, x_f) \in M \\ 1 & \text{otherwise} . \end{cases} \quad (4.36)$$

It is illustrated at Figure 4.7. The expression (4.35) is incorrect for vertices  $\mathbf{x}_i, \mathbf{x}_f$  located

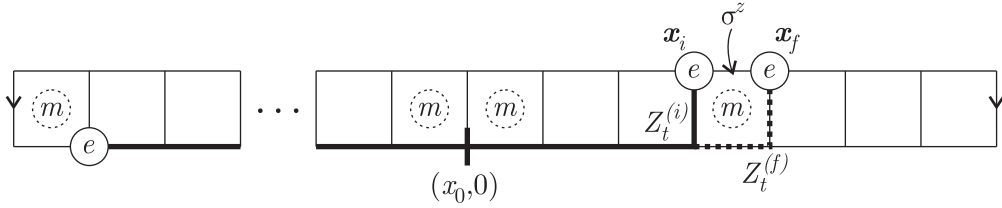


Figure 4.7: The factor  $s(\mathbf{x}_i, \mathbf{x}_f) = -1$  in the case depicted due to the nontrivial braiding properties between  $e$  and  $m$ -type anyons (recall Fig.4.3).

horizontally opposite of  $(x_0, 0)$  since then topologically nontrivial loops can be formed. We will neglect this fact as it does not affect our point — whether the particle remains localized around  $(x_0, 0)$  or spreads. Otherwise we would have to restrict ourselves to a certain neighborhood of  $(x_0, 0)$  with boundaries which would make our analysis much more technical.

The time evolution of the system is governed by the evolution operator  $U^I(t) = e^{itH^I}$ . Since  $H_v^I$  and  $H_p^I$  are just multiples of the identity operator,  $U^I(t)$  factorizes as<sup>8</sup>

$$U^I(t) = e^{it(H_v^I + H_p^I + H_e^I)} = e^{itH_v^I} e^{itH_p^I} e^{itH_e^I} . \quad (4.37)$$

<sup>8</sup>We use the fact that  $e^{A+B} = e^A e^B$  if the commutator  $[A, B] = 0$ .



## 4.4 Continuous-time quantum walks in one dimension

We will analyze the quantum evolution of a particle living on a one dimensional lattice. In literature, especially in the quantum information theory, this problem is called the *continuous-time quantum walk* [35]. Indeed, it is inspired by the classical random walk and translates it into the quantum mechanical framework.

While the time we take continuous, the space is considered discrete. This can be thought of as a tight binding approximation — the particle is anchored to a vertex by a sufficiently deep and thin potential well.

### 4.4.1 Cyclic lattice

Let us consider a free spinless quantum particle moving on a cycle graph with  $N$  vertices (Fig.4.9). The Hilbert space of this system is  $N$ -dimensional,

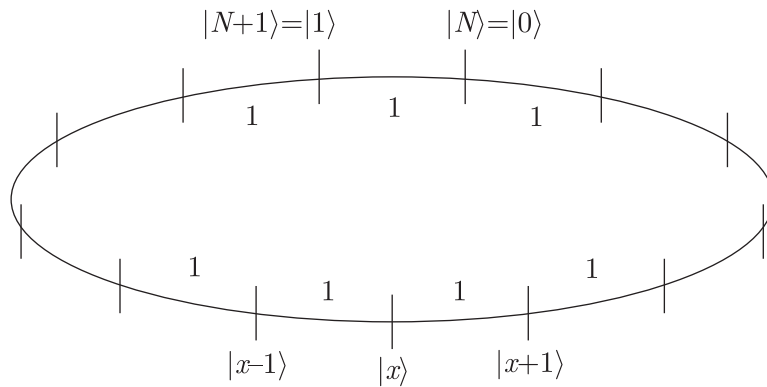


Figure 4.9: The particle moves on a one dimensional periodic lattice pictured as a cycle graph with  $N$  vertices. The hopping amplitudes for all neighboring sites are all equal to 1 (there is no disorder).

$$\mathcal{H} = \text{span}\{|x\rangle\}_{x=1}^N, \quad (4.43)$$

where  $|x\rangle$  are the normalized eigenvectors of the position operator,  $\hat{X}|x\rangle = x|x\rangle$ . We impose periodic boundary conditions  $|x = N + 1\rangle = |x = 1\rangle$  and  $|x = 0\rangle = |x = N\rangle$  and consider the Hamiltonian

$$H = - \sum_{x=1}^N (|x+1\rangle\langle x| + |x\rangle\langle x+1|), \quad (4.44)$$

that is

$$H|x\rangle = -(|x-1\rangle + |x+1\rangle) . \quad (4.45)$$

In the  $|x\rangle$  basis  $H$  takes the matrix form

$$H = \begin{pmatrix} & 1 & & & 1 \\ 1 & & 1 & & \\ & 1 & & \ddots & \\ & & \ddots & & 1 \\ & & & 1 & 1 \\ 1 & & & & 1 \end{pmatrix} . \quad (4.46)$$

This Hamiltonian describes a particle hopping on a one dimensional periodic lattice with the ‘‘hopping amplitude’’ being 1 for all neighboring sites.

The translational symmetry of the problem suggests that using the Fourier transform (i.e. switching to the momentum basis) could lead to simplification. We define for all  $k = 0, \dots, N-1$

$$|k\rangle := \frac{1}{\sqrt{N}} \sum_{x=1}^N e^{i\frac{2\pi}{N}kx} |x\rangle . \quad (4.47)$$

It is easy to see that the  $|k\rangle$  vectors are orthogonal,

$$\langle k|k'\rangle = \frac{1}{N} \sum_{x,x'} e^{i\frac{2\pi}{N}(k'x'-kx)} \underbrace{\langle x|x'\rangle}_{\delta_{xx'}} = \frac{1}{N} \sum_{x=1}^N e^{i\frac{2\pi}{N}(k'-k)x} = \delta_{kk'} , \quad (4.48)$$

and that they are in fact the eigenvectors of the Hamiltonian  $H$ :

$$\begin{aligned} H|k\rangle &= \frac{-1}{\sqrt{N}} \sum_x e^{i\frac{2\pi}{N}kx} (|x+1\rangle + |x-1\rangle) \\ &= \frac{-1}{\sqrt{N}} e^{-i\frac{2\pi}{N}k} \sum_x e^{i\frac{2\pi}{N}k(x+1)} |x+1\rangle + \frac{-1}{\sqrt{N}} e^{i\frac{2\pi}{N}k} \sum_x e^{i\frac{2\pi}{N}k(x-1)} |x-1\rangle \\ &= -e^{-i\frac{2\pi}{N}k} |k\rangle - e^{i\frac{2\pi}{N}k} |k\rangle = -2 \cos\left(\frac{2\pi}{N}k\right) |k\rangle . \end{aligned} \quad (4.49)$$

The eigenvalues  $E_k = -2 \cos\left(\frac{2\pi}{N}k\right)$  are in general twice degenerate,  $E_k = E_{N-k}$ , except for the non-degenerate ground state  $|k=0\rangle = \frac{1}{\sqrt{N}} \sum_x |x\rangle$  and the special case when  $N$  is even and  $k = \frac{N}{2}$ . We have solved the spectral problem of the Hamiltonian  $H$  and thus opened the possibility of finding the time evolution of the system analytically.

Let the particle start at time  $t = 0$  in a fully localized state  $|\psi(0)\rangle = |x = x_0\rangle$ . We are interested in the position distribution of the particle after a time  $t$

$$P_t(x; x_0) = \langle x|\psi(t)\rangle \langle \psi(t)|x\rangle = |\langle x|U(t)|x_0\rangle|^2 , \quad (4.50)$$

where  $|\psi(t)\rangle = U(t)|\psi(0)\rangle$  and  $U(t) = e^{-itH}$  is the evolution operator. For this sake we calculate the amplitude of transition from the state  $|x_0\rangle$  to the state  $|x\rangle$  in time  $t$  using the resolution of unity in terms of the eigenvectors of  $H - \mathbb{1} = \sum_{k=0}^{N-1} |k\rangle\langle k|$ . We obtain

$$\begin{aligned}\langle x|U(t)|x_0\rangle &= \langle x|e^{-itH}|x_0\rangle = \sum_k e^{-itE_k} \langle x|k\rangle\langle k|x_0\rangle \\ &= \frac{1}{N} \sum_{k=0}^{N-1} e^{i2t \cos(\frac{2\pi}{N}k)} e^{i\frac{2\pi}{N}k(x-x_0)} .\end{aligned}\quad (4.51)$$

We can now plug these transition amplitudes into (4.50) to find the position distribution  $P_t(x; x_0)$ . The result is plotted at Fig.4.12 for  $N = 200$ ,  $x_0 = 100$  and times  $t = 20, 50$ . The particle is spread around the cycle when  $t$  is large enough.

We can derive (4.51) using a rather different approach — without diagonalizing the Hamiltonian. Starting with

$$\langle x|U(t)|x_0\rangle = \langle x|e^{-itH}|x_0\rangle \quad (4.52)$$

and expanding the exponential,

$$\langle x|e^{-itH}|x_0\rangle = \sum_{n=0}^{\infty} \frac{(it)^n}{n!} \langle x|(-H)^n|x_0\rangle , \quad (4.53)$$

we realize that the terms  $\langle x|(-H)^n|x_0\rangle$  answer a classical question: How many ways can a classical particle (a *drunken sailor*) walking on a cycle graph with  $N$  vertices get in  $n$ -steps from the point  $x_0$  to the point  $x$ . Due to the periodicity of the cycle we have

$$\langle x|(-H)^n|x_0\rangle = \sum_{p \in \mathbb{Z}} \binom{n}{\frac{x+pN-x_0}{2} + \frac{n}{2}} , \quad (4.54)$$

where we use the usual convention that  $\binom{n}{k} = 0$  if  $k \notin \{0, 1, \dots, n\}$ . We rewrite the latter in terms of the Kronecker  $\delta$  symbol,

$$\langle x|(-H)^n|x_0\rangle = \sum_{p \in \mathbb{Z}} \sum_{j=0}^n \binom{n}{j} \delta_{2j, x+pN-x_0+n} = \sum_{j=0}^n \binom{n}{j} \sum_{p \in \mathbb{Z}} \delta_{2j, x+pN-x_0+n} \quad (4.55)$$

and use the relation

$$\frac{1}{N} \sum_{k=0}^{N-1} e^{i\frac{2\pi}{N}k(r-s)} = \begin{cases} 1 & \text{if } r = s + pN \text{ for some } p \in \mathbb{Z} \\ 0 & \text{otherwise} \end{cases} \quad (4.56)$$

to obtain

$$\begin{aligned}
\langle x|(-H)^n|x_0\rangle &= \sum_{j=0}^n \binom{n}{j} \frac{1}{N} \sum_{k=0}^{N-1} e^{i\frac{2\pi}{N}k(x-x_0+n-2j)} \\
&= \frac{1}{N} \sum_{k=0}^{N-1} e^{i\frac{2\pi}{N}k(x-x_0)} \sum_{j=0}^n \binom{n}{j} e^{i\frac{2\pi}{N}k(n-j)} e^{-i\frac{2\pi}{N}kj} \\
&= \frac{1}{N} \sum_{k=0}^{N-1} e^{i\frac{2\pi}{N}k(x-x_0)} \left( e^{i\frac{2\pi}{N}k} + e^{-i\frac{2\pi}{N}k} \right)^n \\
&= \frac{1}{N} \sum_{k=0}^{N-1} e^{i\frac{2\pi}{N}k(x-x_0)} \left( 2 \cos \frac{2\pi}{N}k \right)^n .
\end{aligned} \tag{4.57}$$

Plugging this back into (4.53), the transition amplitudes read

$$\begin{aligned}
\langle x|U(t)|x_0\rangle &= \sum_{n=0}^{\infty} \frac{(it)^n}{n!} \langle x|(-H)^n|x_0\rangle \\
&= \frac{1}{N} \sum_{k=0}^{N-1} e^{i\frac{2\pi}{N}k(x-x_0)} e^{i2t \cos(\frac{2\pi}{N}k)} ,
\end{aligned} \tag{4.58}$$

which, indeed, equals (4.51).

## 4.4.2 Infinite line

What happens if we send  $N \rightarrow \infty$ ? This corresponds to replacing a finite circle by an infinite line.<sup>9</sup> The sum in (4.51) is replaced by an integral,  $\frac{k}{N}$  by  $z$  and  $\frac{1}{N}$  by  $dz$ . The transition amplitudes read

$$\langle x|U(t)|x_0\rangle|_{N \rightarrow \infty} = \int_0^1 e^{i2t \cos(2\pi z)} e^{i2\pi z(x-x_0)} dz = \frac{1}{2\pi} \int_0^{2\pi} e^{i2t \cos z} e^{iz(x-x_0)} dz , \tag{4.59}$$

where now  $x_0, x \in \mathbb{Z}$ . After the substitution  $z \rightarrow -z + \frac{\pi}{2}$  and using the fact that the integrated function is  $2\pi$ -periodic,

$$\frac{1}{2\pi} \int_0^{2\pi} e^{i2t \cos z} e^{iz(x-x_0)} dz = \frac{i^{x-x_0}}{2\pi} \int_0^{2\pi} e^{i2t \sin z} e^{-iz(x-x_0)} dz \tag{4.60}$$

and we unveil the integral representation of the Bessel functions of the first kind ([36], formula 8.411.1). This gives the transition amplitudes a compact form

$$\langle x|U(t)|x_0\rangle|_{N \rightarrow \infty} = i^{x-x_0} J_{x-x_0}(2t) . \tag{4.61}$$

---

<sup>9</sup>It is important that we carry out the limit  $N \rightarrow \infty$  at the beginning and not only work in a large (but finite)  $N$  regime, where our following conclusions would be valid merely for  $x - x_0$  and  $t$  small enough compare to  $N$ .

The position distribution of the particle in the  $N \rightarrow \infty$  limit then takes the form

$$P_t(x; x_0)|_{N \rightarrow \infty} = |\langle x|U(t)|x_0 \rangle|_{N \rightarrow \infty}^2 = (J_{x-x_0}(2t))^2 . \quad (4.62)$$

It is plotted in Figure 4.10(a).

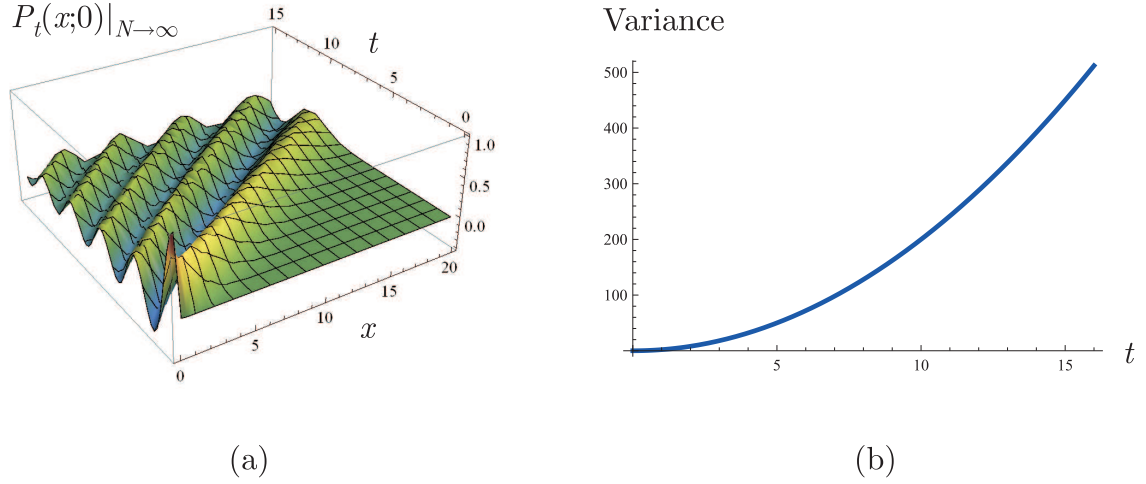


Figure 4.10: (a) The position distribution  $P_t(x; 0)|_{N \rightarrow \infty}$  of a particle walking on the infinite line graph, initially localized at position  $x_0 = 0$ , is shown for the time interval  $t \in [0, 15]$  and the sites  $x \in \{0, \dots, 20\}$  ( $P_t(x; 0)|_{N \rightarrow \infty}$  is symmetric with respect to  $x_0$ ). (b) The variance of the distribution  $P_t(x; 0)|_{N \rightarrow \infty}$  grows quadratically with  $t$ .

Let us put  $x_0 = 0$  for simplicity. The moments of the probability distribution  $P_t(x; 0)|_{N \rightarrow \infty}$ ,

$$\langle X^m \rangle(t) = \sum_{x=-\infty}^{\infty} x^m (J_x(2t))^2 , \quad (4.63)$$

can be expressed in the following way. For the Bessel  $J$  function it holds that

$$e^{\pm i 2t \sin z} = \sum_{x=-\infty}^{\infty} J_x(2t) e^{\pm i x z} \quad (4.64)$$

([36], formula 8.511.4). We may write

$$\begin{aligned}
\langle X^m \rangle(t) &= \sum_{x=-\infty}^{\infty} \sum_{x'=-\infty}^{\infty} x^m J_x(2t) J_{x'}(2t) \underbrace{\frac{1}{2\pi} \int_0^{2\pi} e^{-ix'z} e^{ixz} dz}_{\delta_{x,x'}} \\
&= \sum_{x=-\infty}^{\infty} \sum_{x'=-\infty}^{\infty} J_x(2t) J_{x'}(2t) \frac{1}{2\pi} \int_0^{2\pi} e^{-ix'z} (-i)^m \frac{\partial^m}{\partial z^m} e^{ixz} dz \\
&= \frac{1}{2\pi} \int_0^{2\pi} \left( \sum_{x'=-\infty}^{\infty} J_{x'}(2t) e^{-ix'z} \right) (-i)^m \frac{\partial^m}{\partial z^m} \left( \sum_{x=-\infty}^{\infty} J_x(2t) e^{ixz} \right) dz \quad (4.65)
\end{aligned}$$

and using (4.64) we derive

$$\langle X^m \rangle(t) = \frac{(-i)^m}{2\pi} \int_0^{2\pi} e^{-i2t \sin z} \frac{\partial^m}{\partial z^m} e^{i2t \sin z} dz . \quad (4.66)$$

It is not difficult to calculate first few moments explicitly:

$$\langle X^0 \rangle(t) = 1 \quad (4.67)$$

reflects a proper normalization of the probability distribution;

$$\langle X^1 \rangle(t) = 0 \quad (4.68)$$

is the mean value (generally,  $\langle X^1 \rangle(t) = x_0$ );

$$\langle X^2 \rangle(t) = 2t^2 \quad (4.69)$$

is in our case equal to the variance  $\langle X^2 \rangle - \langle X \rangle^2$ , which measures the spreading (or delocalization) of the particle (Fig.4.10(b));

$$\langle X^3 \rangle(t) = 0 , \quad (4.70)$$

$$\langle X^4 \rangle(t) = 2t^2(1 + 3t^2) , \text{ etc } \dots \quad (4.71)$$

In general,  $\langle X^{2m+1} \rangle(t) = 0$  for all  $m \in \mathbb{N}$  since  $P_t(x; 0)|_{N \rightarrow \infty}$  is an even function of  $x$ .<sup>10</sup>

An explicit calculation of the even moments  $\langle X^{2m} \rangle(t)$ ,  $m \in \mathbb{N}$ , requires to perform repeated differentiation of a composite function. However, we can easily (with the aid of [36], formula 3.621.3) find at least the leading term of  $\langle X^{2m} \rangle(t)$  for arbitrary  $m$ :

$$\begin{aligned}
\langle X^{2m} \rangle(t) &= \frac{(-i)^{2m}}{2\pi} \int_0^{2\pi} (i2t)^{2m} (\cos z)^{2m} dz + \dots \text{ (lower orders of } t) \\
&= \binom{2m}{m} t^{2m} + \dots . \quad (4.72)
\end{aligned}$$

---

<sup>10</sup>It holds that

$$J_{-n}(t) = (-1)^n J_n(t)$$

for  $n \in \mathbb{Z}$ .

### 4.4.3 Cyclic lattice with disordered couplings

We can generalize the previous model by allowing the “hopping amplitudes” for neighboring sites to take values  $+1$  or  $-1$  (Fig.4.11). We hence get a family of Hamiltonians

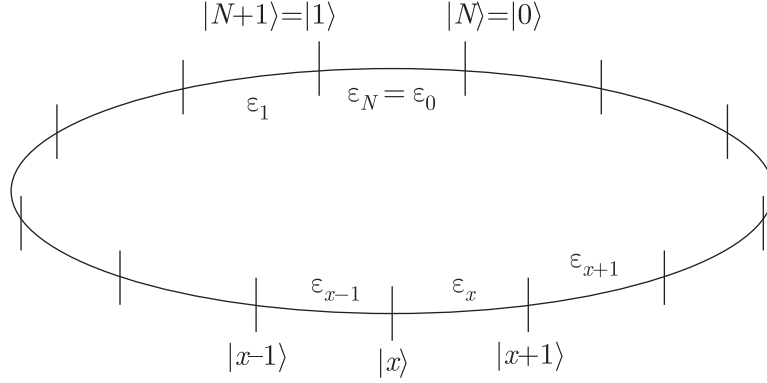


Figure 4.11: The particle moves on a one dimensional periodic lattice with  $N$  sites. The hopping amplitudes are allowed to take values  $\varepsilon_j = \pm 1, j = 1, \dots, N$ .

$$H_{\vec{\varepsilon}} = - \sum_{x=1}^N \varepsilon_x (|x+1\rangle\langle x| + |x\rangle\langle x+1|) , \quad (4.73)$$

or

$$H_{\vec{\varepsilon}}|x\rangle = -(\varepsilon_{x-1}|x-1\rangle + \varepsilon_x|x+1\rangle) , \quad (4.74)$$

characterized by binary vectors

$$\vec{\varepsilon} = (\varepsilon_1, \varepsilon_2, \dots, \varepsilon_N) , \quad \varepsilon_j \in \{-1, 1\} . \quad (4.75)$$

The boundary conditions are again periodic,  $|x = N + 1\rangle = |x = 1\rangle$  and  $|x = 0\rangle = |x = N\rangle$ , and we define  $\varepsilon_0 := \varepsilon_N$ . Note that the undisordered Hamiltonian (4.44) is contained in this family as the special case  $\vec{\varepsilon} = (1, \dots, 1) \equiv \vec{1}$ .

We shall see that the generalized problem is solvable for any configuration  $\vec{\varepsilon}$ . Well, let us try to solve the spectral problem for  $H_{\vec{\varepsilon}}$ ,

$$H_{\vec{\varepsilon}}|\psi\rangle = E|\psi\rangle , \quad (4.76)$$

which leads to the set of  $N$  equations

$$-\varepsilon_{x-1}\langle x-1|\psi\rangle - \varepsilon_x\langle x+1|\psi\rangle = E\langle x|\psi\rangle , \quad x = 1, \dots, N \quad (4.77)$$

for the components of  $|\psi\rangle$  in the  $X$ -representation. We may regard this as a linear recurrence relation for a finite sequence  $\{\langle x|\psi\rangle\}_{x=0}^{N+1}$  subject to the boundary conditions

$$\begin{aligned}\langle 0|\psi\rangle &= \langle N|\psi\rangle \\ \langle N+1|\psi\rangle &= \langle 1|\psi\rangle .\end{aligned}\tag{4.78}$$

After multiplying (4.77) by  $\prod_{j=x}^N \varepsilon_j$  and rearranging the terms we face (keep in mind that  $\varepsilon_x^2 = 1$  for all  $x$ )

$$\left(\prod_{j=x+1}^N \varepsilon_j\right) \langle x+1|\psi\rangle + E \left(\prod_{j=x}^N \varepsilon_j\right) \langle x|\psi\rangle + \left(\prod_{j=x-1}^N \varepsilon_j\right) \langle x-1|\psi\rangle = 0, \quad x = 1, \dots, N. \tag{4.79}$$

Now, for  $\vec{\varepsilon} = \vec{1}$  we know that the Hamiltonian is the one without disorder and its eigenvectors are given by (4.47). Fortunately, we can get rid of the  $\vec{\varepsilon}$  dependence in the recurrence (4.79) by making the ansatz

$$\langle x|\psi\rangle = \left(\prod_{j=x}^N \varepsilon_j\right) e^{i\frac{2\pi}{N}\omega x}, \quad x = 0, \dots, N+1. \tag{4.80}$$

(We use the usual convention  $\prod_{j=a}^b (\dots) = 1$  if  $a > b$ .) One can easily convince oneself that such  $|\psi\rangle$  satisfies the equations (4.79) provided that

$$E = -2 \cos\left(\frac{2\pi}{N}\omega\right). \tag{4.81}$$

The parameter  $\omega$  is restricted by the boundary conditions (4.78) that for our choice of  $|\psi\rangle$  read

$$\left(\prod_{j=0}^N \varepsilon_j\right) = \varepsilon_N e^{i2\pi\omega} \tag{4.82}$$

$$e^{i\frac{2\pi}{N}\omega(N+1)} = \left(\prod_{j=1}^N \varepsilon_j\right) e^{i\frac{2\pi}{N}\omega}. \tag{4.83}$$

Since, by definition,  $\varepsilon_0 = \varepsilon_N$ , these two conditions are equivalent and yield

$$e^{i2\pi\omega} = \text{sgn}(\vec{\varepsilon}), \tag{4.84}$$

where we denoted

$$\text{sgn}(\vec{\varepsilon}) \equiv \prod_{j=1}^N \varepsilon_j = \pm 1. \tag{4.85}$$

If  $\text{sgn}(\vec{\varepsilon}) = +1$ ,

$$\omega = k, \quad k = 0, \dots, N-1. \quad (4.86)$$

The eigenvalues of  $H_{\vec{\varepsilon}}$  are

$$E_k^+ = -2 \cos\left(\frac{2\pi}{N}k\right), \quad k = 0, \dots, N-1 \quad (4.87)$$

and the (orthonormal) eigenvectors of  $H_{\vec{\varepsilon}}$  read

$$|k^{+\varepsilon}\rangle = \frac{1}{\sqrt{N}} \sum_{x=1}^N \left( \prod_{j=x}^N \varepsilon_j \right) e^{i\frac{2\pi}{N}kx} |x\rangle, \quad k = 0, \dots, N-1. \quad (4.88)$$

If  $\text{sgn}(\vec{\varepsilon}) = -1$ ,

$$\omega = k + \frac{1}{2}, \quad k = 0, \dots, N-1. \quad (4.89)$$

The eigenvalues of  $H_{\vec{\varepsilon}}$  are

$$E_k^- = -2 \cos\left(\frac{2\pi}{N}k + \frac{\pi}{N}\right), \quad k = 0, \dots, N-1 \quad (4.90)$$

and the (orthonormal) eigenvectors of  $H_{\vec{\varepsilon}}$  read

$$|k^{-\varepsilon}\rangle = \frac{1}{\sqrt{N}} \sum_{x=1}^N \left( \prod_{j=x}^N \varepsilon_j \right) e^{i\frac{\pi}{N}x} e^{i\frac{2\pi}{N}kx} |x\rangle, \quad k = 0, \dots, N-1. \quad (4.91)$$

Let's check the orthonormality of the vectors  $|k^{+\varepsilon}\rangle$ :

$$\langle k_1^{+\varepsilon} | k_2^{+\varepsilon} \rangle = \frac{1}{N} \sum_{x_1, x_2} \left( \prod_{j=x_1}^N \varepsilon_j \right) \left( \prod_{j=x_2}^N \varepsilon_j \right) e^{-i\frac{2\pi}{N}k_1x_1} e^{i\frac{2\pi}{N}k_2x_2} \langle x_1 | x_2 \rangle \quad (4.92)$$

$$= \frac{1}{N} \sum_{x_1} e^{i\frac{2\pi}{N}(k_2-k_1)x_1} = \delta_{k_1, k_2}. \quad (4.93)$$

In the same way we can prove the orthonormality of the vectors  $|k^{-\varepsilon}\rangle$ .

Once the eigenvectors are known, it is easy to probe the time evolution of the system. Depending on  $\text{sgn}(\vec{\varepsilon})$ , the transition amplitudes are either

$$\begin{aligned} \langle x | U_{+\varepsilon}(t) | x_0 \rangle &= \langle x | e^{-itH_{\vec{\varepsilon}}} | x_0 \rangle = \sum_k e^{-itE_k^{+\varepsilon}} \langle x | k^{+\varepsilon} \rangle \langle k^{+\varepsilon} | x_0 \rangle \\ &= \frac{1}{N} \left( \prod_{j=x}^N \varepsilon_j \right) \left( \prod_{j=x_0}^N \varepsilon_j \right) \sum_{k=1}^N e^{i2t \cos\left(\frac{2\pi}{N}k\right)} e^{i\frac{2\pi}{N}k(x-x_0)} \end{aligned} \quad (4.94)$$

for  $\text{sgn}(\vec{\varepsilon}) = +1$ , or

$$\begin{aligned} \langle x|U_{-\varepsilon}(t)|x_0\rangle &= \langle x|e^{-itH_{\vec{\varepsilon}}}|x_0\rangle = \sum_k e^{-itE_k^{-\varepsilon}} \langle x|k^{-\varepsilon}\rangle \langle k^{-\varepsilon}|x_0\rangle \\ &= \frac{1}{N} \left( \prod_{j=x}^N \varepsilon_j \right) \left( \prod_{j=x_0}^N \varepsilon_j \right) e^{i\frac{\pi}{N}(x-x_0)} \sum_{k=1}^N e^{i2t \cos(\frac{2\pi}{N}k + \frac{\pi}{N})} e^{i\frac{2\pi}{N}k(x-x_0)} \end{aligned} \quad (4.95)$$

for  $\text{sgn}(\vec{\varepsilon}) = -1$ . To obtain the position distribution after time  $t$ , starting with a localized state  $|\psi(0)\rangle = |x_0\rangle$ , we calculate the modulus squared of the transition amplitudes (4.94) and (4.95). Clearly, the results only depend on  $\text{sgn}(\vec{\varepsilon})$ , not on the details  $\varepsilon_j$  of the particular configuration  $\vec{\varepsilon}$ :

$$\begin{aligned} P_t^+(x; x_0) &= \frac{1}{N^2} \left| \sum_{k=1}^N e^{i2t \cos(\frac{2\pi}{N}k)} e^{i\frac{2\pi}{N}k(x-x_0)} \right|^2 && \text{for } \text{sgn}(\vec{\varepsilon}) = +1, \\ P_t^-(x; x_0) &= \frac{1}{N^2} \left| \sum_{k=1}^N e^{i2t \cos(\frac{2\pi}{N}k + \frac{\pi}{N})} e^{i\frac{2\pi}{N}k(x-x_0)} \right|^2 && \text{for } \text{sgn}(\vec{\varepsilon}) = -1. \end{aligned} \quad (4.96)$$

The position distributions  $P_t^+(x; x_0)$  and  $P_t^-(x; x_0)$  are plotted at Fig.4.12 and Fig.4.13, respectively, for the cycle of length  $N = 200$ , the initial state  $|x_0\rangle = |100\rangle$ , and times  $t = 20, 50$ . The particle (initially fully localized) spreads around the cycle, i.e. its localization is lost. This holds for both  $\text{sgn}(\vec{\varepsilon}) = +1$  and  $-1$  and the corresponding plots are in fact hardly told apart by eye.

**Remark:** Yet, it can be important whether we have  $\vec{\varepsilon}$  such that  $\text{sgn}(\vec{\varepsilon}) = +1$  or  $-1$ . Consider two simple examples of cycles of size  $N = 4$  with the hopping amplitudes as pictured in Fig.4.14. Let us choose the initial state  $|x_0\rangle = |1\rangle$  and calculate the particle's distribution after a time  $t$ . For each site  $|x\rangle$  we obtain a function of  $t$ ,  $P_t^\pm(x; x_0)$ . The results for (a)  $\text{sgn}(\vec{\varepsilon}) = +1$  and (b)  $\text{sgn}(\vec{\varepsilon}) = -1$  are plotted at Fig.4.15(a) and (b), respectively.

The interference phenomena change dramatically the propagation of the particle. In particular, in the case (b) the particle can never (for no  $t$ ) be found at the opposite corner of the square (position  $|x = 3\rangle$ ). This is because the particle's histories traveling from  $|1\rangle$  to  $|3\rangle$  via  $|2\rangle$  pick up phases opposite to those traveling via  $|4\rangle$ .

## 4.5 Numerical results for one anyon walk on a periodic ladder lattice

We have seen in the previous section that a particle living on a one dimensional lattice with nearest neighbour interaction tends to spread for any choice of disorder  $\vec{\varepsilon}$  in the

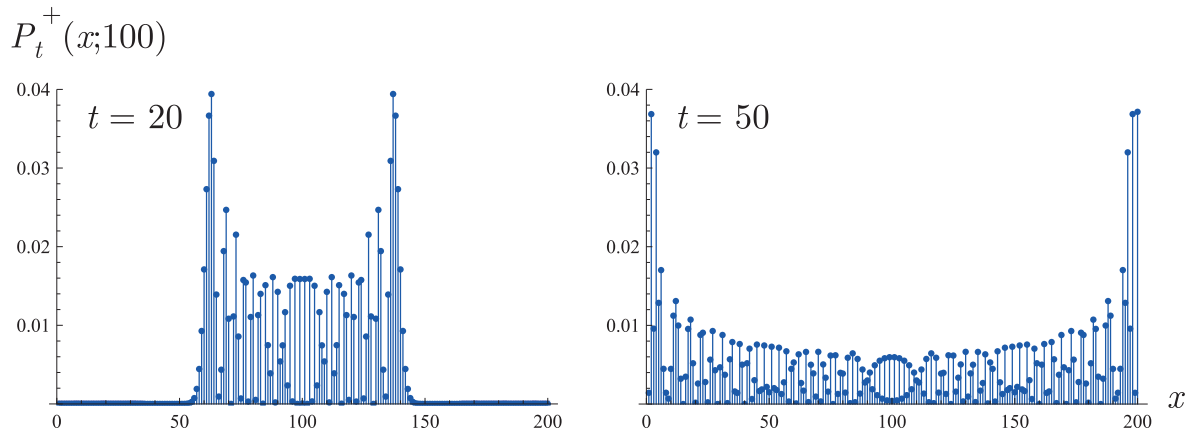


Figure 4.12: The position distribution  $P_t^+(x;100)$  of a particle evolving on a cycle graph with  $N = 200$  vertices, from the initially localized state  $|x = 100\rangle$ . The disorder of the Hamiltonian  $H_{\vec{\varepsilon}}$  is characterized by the vector  $\vec{\varepsilon}$  with  $\text{sgn}(\vec{\varepsilon}) = +1$ . Two time instances are shown:  $t = 20$  and  $t = 50$ .

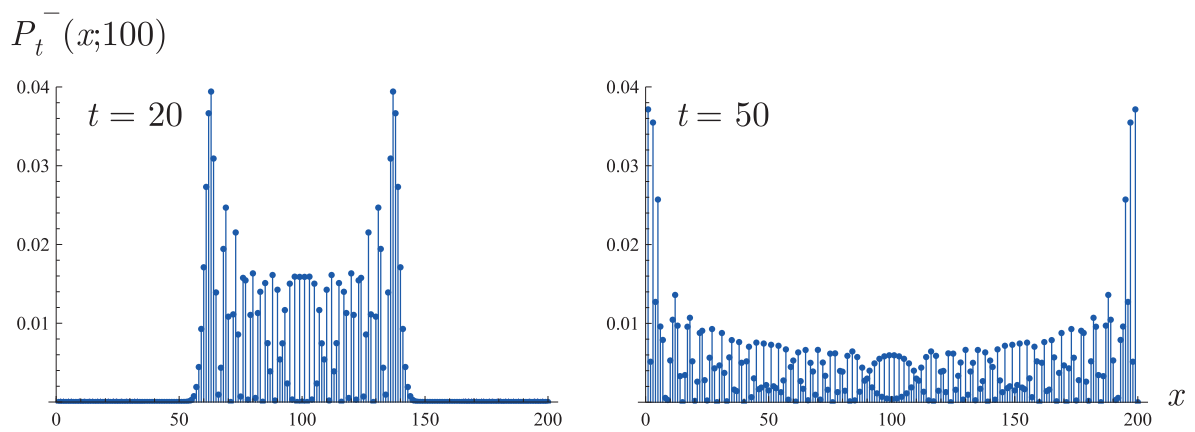


Figure 4.13: The position distribution  $P_t^-(x;100)$  of a particle evolving on a cycle graph with  $N = 200$  vertices, from the initially localized state  $|x = 100\rangle$ . The disorder of the Hamiltonian  $H_{\vec{\varepsilon}}$  is characterized by the vector  $\vec{\varepsilon}$  with  $\text{sgn}(\vec{\varepsilon}) = -1$ . Two time instances are shown:  $t = 20$  and  $t = 50$ .

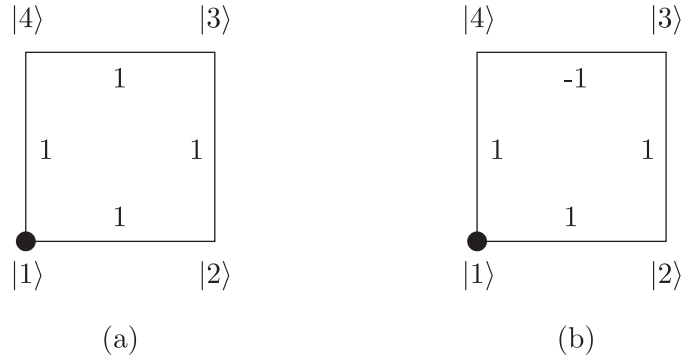


Figure 4.14: (a) A lattice corresponding to  $\vec{\varepsilon} = (1, 1, 1, 1)$ ,  $\text{sgn}(\vec{\varepsilon}) = +1$ . (b) A lattice with hopping amplitudes corresponding to  $\vec{\varepsilon} = (1, 1, -1, 1)$ ,  $\text{sgn}(\vec{\varepsilon}) = -1$ . The initial state is  $|x_0\rangle = |1\rangle$ .

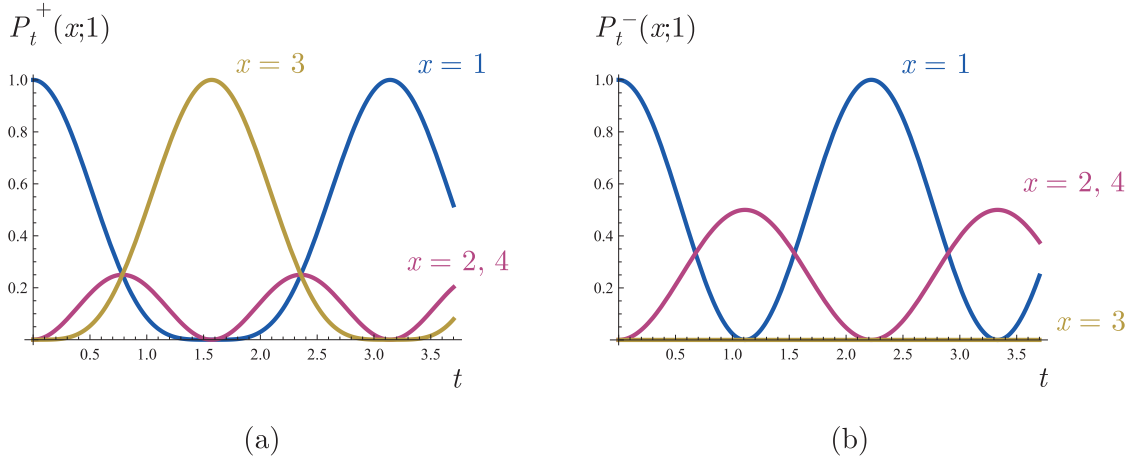


Figure 4.15: The probabilities of finding a particle initiated at vertex  $|1\rangle$  on a square lattice (see Fig.4.14) are plotted as functions of time  $t$  for various sites  $|x\rangle$ . (a) The case when  $\text{sgn}(\vec{\varepsilon}) = +1$ . (b) The case when  $\text{sgn}(\vec{\varepsilon}) = -1$ . The two cases differ most significantly at the site  $|3\rangle$ .

Hamiltonian  $H_{\vec{\varepsilon}}$  (4.73), specially for the Hamiltonian  $H_0$  (4.44). For an infinite lattice, the variance of the resulting position distribution grows as  $\sim t^2$  (4.69). In the finite case, when  $N$  is the number of sites of the periodic lattice, this quadratic dependence holds until the spreading wave function starts to interfere with itself as the two parts propagating in opposite directions meet and mix together.

We have also seen that the presence of  $-1$  hopping terms in the Hamiltonian causes

destructive interference (recall Fig.4.15) that can play an important role for small cycles, where the wave function mixes almost immediately.

For the periodic ladder lattice (4.8) these two attributes coexist. Since for a general configuration of the  $m$  anyons we are unable to diagonalize the corresponding Hamiltonian (4.38) analytically, we turn to numerics.

### 4.5.1 Regular disorder – delocalization

Let us first consider the case of regularly placed  $m$  anyons. Suppose there is an  $m$  anyon on every second plaquette. The Hamiltonian  $H_e^I$ , which we will denote simply  $H$  from now on, is of the form

$$H \equiv H_e^I = -h(\mathbf{1} \otimes H_2 + H_0 \otimes |0\rangle\langle 0| + H_{\varepsilon} \otimes |1\rangle\langle 1|) \quad (4.97)$$

with

$$\varepsilon_x = \begin{cases} 1 & \text{if } x \text{ is odd} \\ -1 & \text{if } x \text{ is even} . \end{cases} \quad (4.98)$$

We choose a localized initial state  $|\psi_0\rangle = |x_0\rangle \otimes |0\rangle$  and calculate  $|\psi(t)\rangle = U(t)|\psi_0\rangle$  — the wave function after a time  $t$ . To find  $U(t) = e^{-itH}$ , it is necessary to diagonalize the Hamiltonian  $H$ , i.e. to find a diagonal matrix  $A$  and a transformation matrix  $S$  such that  $H = SAS^{-1}$ . This step is done numerically. We are interested in the position distribution along the horizontal axis of the ladder

$$P_t^{reg}(x; x_0) = \sum_{y=0}^1 \langle x, y | \psi(t) \rangle \langle \psi(t) | x, y \rangle = |\langle x, 0 | U(t) | \psi_0 \rangle|^2 + |\langle x, 1 | U(t) | \psi_0 \rangle|^2 . \quad (4.99)$$

From  $P_t^{reg}(x; x_0)$  we calculate the corresponding variance

$$Var_{reg}(t) = \sum_{x=1}^N x^2 P_t^{reg}(x; x_0) - \left( \sum_{x=1}^N x P_t^{reg}(x; x_0) \right)^2 \quad (4.100)$$

that tells us quantitatively about the spreading of the particle.

The time scale is defined by the perturbation strength  $h$  ( $\hbar = 1$  from the very beginning). It is convenient to introduce the dimensionless time

$$\tau := ht . \quad (4.101)$$

The numerical results are presented for the ladder horizontal size  $N = 200$ , the initial position  $x_0 = 100$  and for  $\tau \in [0, 200]$  with time-step  $\Delta\tau = 1$ . Figure 4.16 shows the

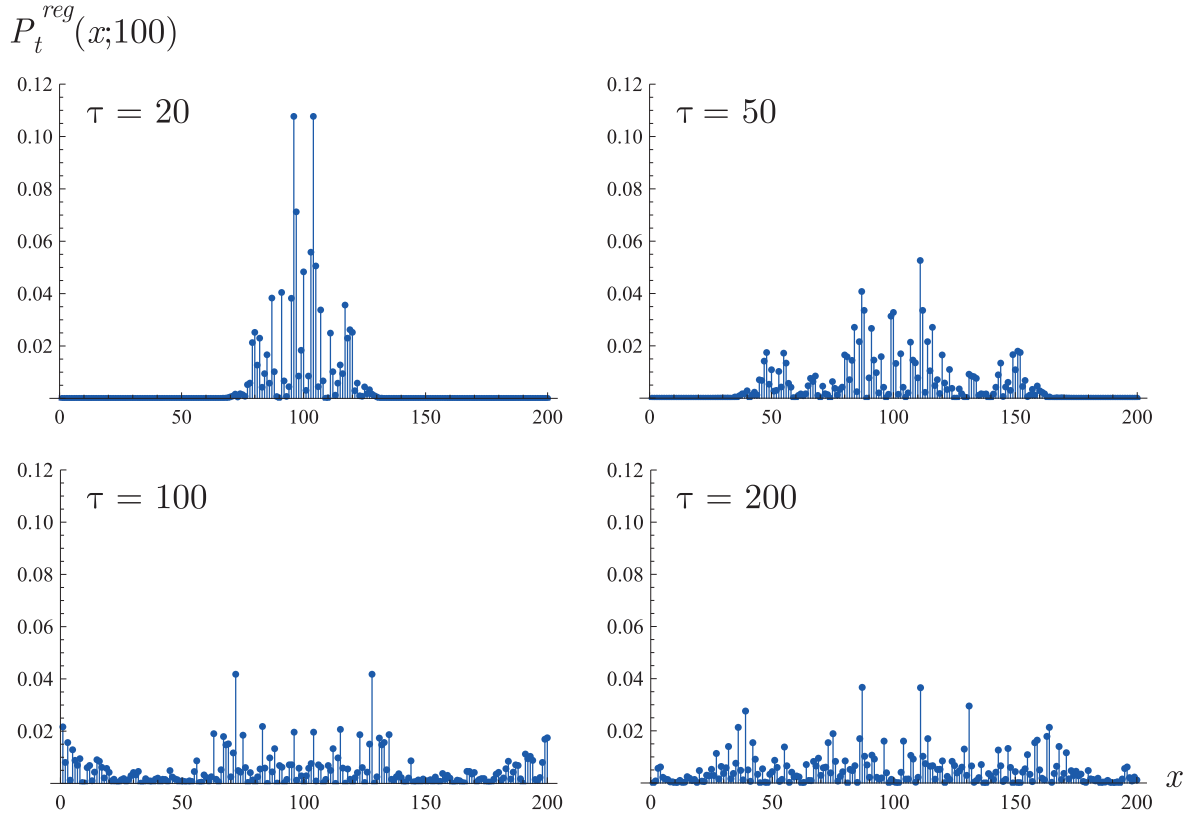


Figure 4.16: The position distributions  $P_t^{reg}(x; 100)$  are shown for  $\tau = 20, 50, 100, 200$ . The particle, initially localized around  $x_0 = 100$ , fills up the ladder about the time  $\tau = 100$ .

position distributions  $P_t^{reg}(x; 100)$  for  $\tau = 20, 50, 100, 200$ , Figure 4.17 illustrates how the variance  $Var_{reg}$  changes with time. At  $\tau = 100$  the variance reaches its maximum value  $Var_{reg} = 3128.14$ . This is comparable to the variance of the uniform distribution  $P^{uni}(x) = \frac{1}{N}$ , which comes out as

$$Var_{uni} = \frac{1}{N} \sum_{x=1}^N x^2 - \left( \frac{1}{N} \sum_{x=1}^N x \right)^2 = \frac{N^2 - 1}{12} = 3333.25 . \quad (4.102)$$

The walker, clearly, gets delocalized — logical error is likely to occur at  $\tau = 100 = \frac{N}{2}$ .

## 4.5.2 Random disorder – localization

More realistically,  $m$  errors occur at random positions, they don't form a regular pattern. We will consider a model in which an  $m$  anyon occupies a given plaquette with probability

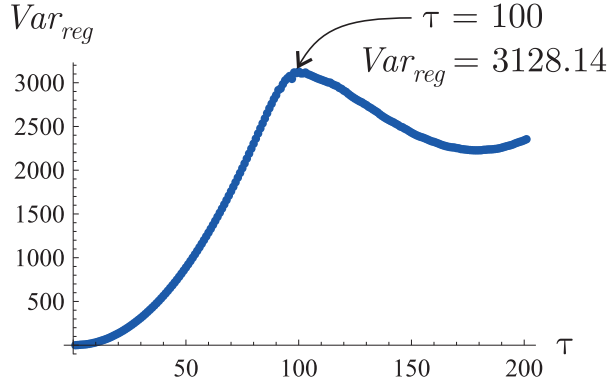


Figure 4.17: The variance of the walker’s position distribution for regularly placed  $m$  anyons,  $Var_{reg}$ , as a function of the dimensionless time  $\tau$  grows as  $\sim \tau^2$  up to the point ( $\tau = 100$ ,  $Var_{reg} = 3128.14$ ) when oppositely propagating parts of the wave function  $|\psi(t)\rangle$  meet.

$\frac{1}{2}$ . This probability is equal for all plaquettes.<sup>11</sup> That is, on average there should be one half of the plaquettes populated. The pattern, however, is random and this fact proves to be fundamental for the motion of the  $e$  anyonic walker.

We are interested in the quantities averaged over all configurations (patterns)  $M \subseteq \{1, \dots, N\}$  of the  $m$  anyons (see (4.30)).  $N$  denotes the number of plaquettes as usually. There are  $2^N$  possible configurations and all of them are realized with the equal probability  $\frac{1}{2^N}$ . Let us start with a localized initial state  $|\psi_0\rangle = |x_0\rangle \otimes |0\rangle$ . The  $M$ -averaged horizontal position distribution of the walker after a time  $t$  reads

$$P_t^{ran}(x; x_0) = \frac{1}{2^N} \sum_{M \subseteq \{1, \dots, N\}} \left( |\langle x, 0 | U^M(t) | \psi_0 \rangle|^2 + |\langle x, 1 | U^M(t) | \psi_0 \rangle|^2 \right), \quad (4.103)$$

where  $U^M(t)$  is the evolution operator corresponding to the Hamiltonian  $H_e^I$  (4.73) with the disorder  $\vec{\varepsilon}$  specified by the particular set  $M$ ,

$$\varepsilon_x = \begin{cases} -1 & \text{if } x \in M \\ 1 & \text{if } x \notin M. \end{cases} \quad (4.104)$$

The  $M$ -averaged variance  $Var_{ran}(t)$  is calculated from  $P_t^{ran}(x; x_0)$  in a standard way,

$$Var_{ran}(t) = \sum_{x=1}^N x^2 P_t^{ran}(x; x_0) - \left( \sum_{x=1}^N x P_t^{ran}(x; x_0) \right)^2. \quad (4.105)$$

<sup>11</sup>This yields a rather dense (and perhaps unrealistic) population of the  $m$  anyons. We want to distill the effect of a random pattern even when the lattice that we are able to probe numerically is rather small. We believe that the effects would be similar for large lattices and sparsely distributed  $m$  anyons.

We present our numerical results, again, for  $N = 200$ ,  $x_0 = 100$  and  $\tau \in [0, 200]$  with  $\Delta\tau = 1$ . Since it is computationally impossible to average over all  $2^{200}$  configurations  $M$ , we randomly chose 1000. The results are shown at Figure 4.18 (position distributions of the walker at  $\tau = 20, 50, 100, 200$ ) and at Figure 4.19 (variance as a function of  $\tau$ ).

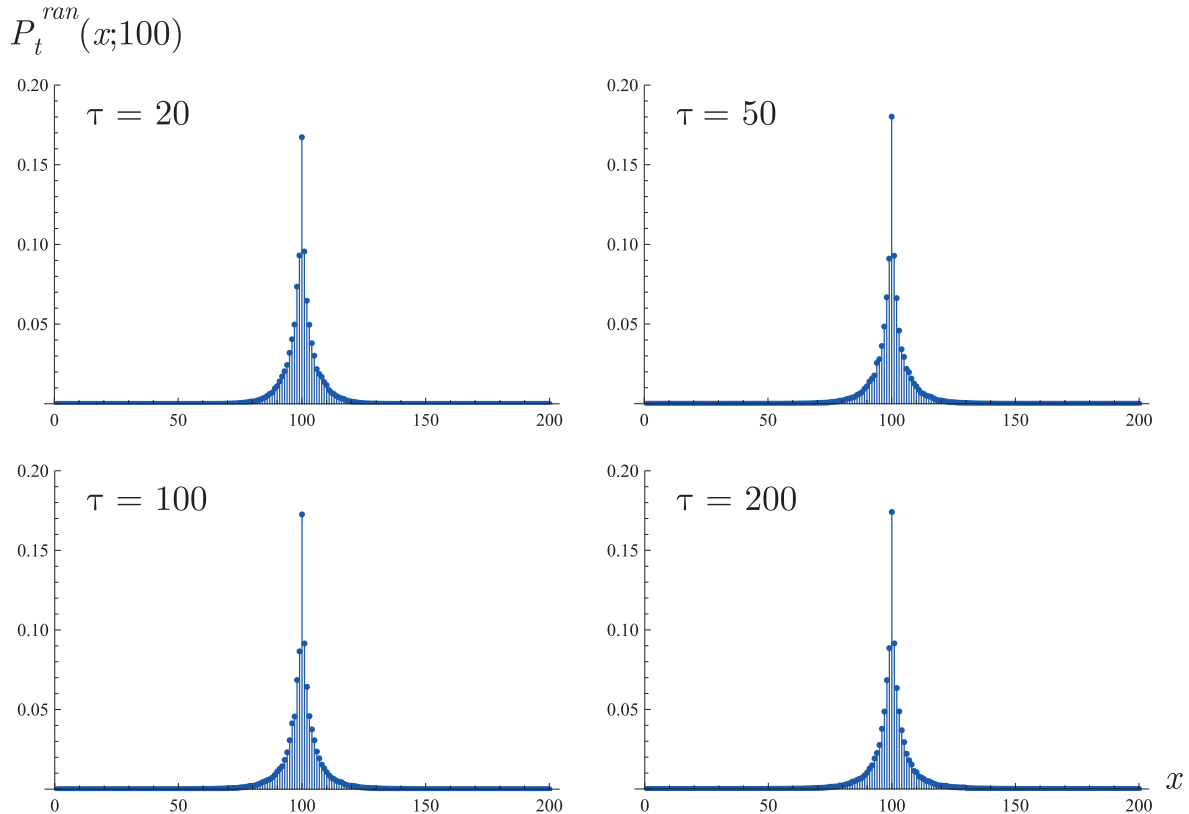


Figure 4.18: The average position distributions in the case of a random disorder,  $P_t^{ran}(x; 100)$ , are shown for  $\tau = 20, 50, 100, 200$ . They don't change significantly with time. The particle remains localized around its initial position  $|x_0\rangle$ .

The walker's position distributions are symmetric and maintain their characteristic shape — one sharp peak at the initial position  $x_0$ . As the distance between  $x$  and  $x_0$  increases, the probability of finding the particle at position  $x$  exponentially decays. This is a general feature of disordered quantum systems known as the *Anderson localization* (see the original Anderson's paper [6] or a recent overview [34]). A quantum particle living in a disordered environment remains localized due to the interference phenomena. Both words — *remains* and *localized* — are important. When exponentially decaying distributions are observed, one also needs to check that the characteristic width of the distribution, the

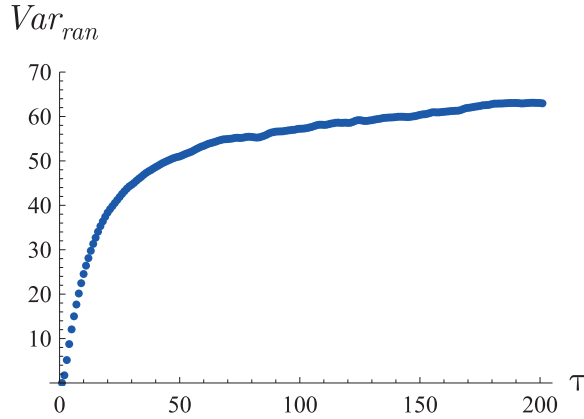


Figure 4.19: The variance of the walker’s position distribution for randomly placed  $m$  anyons,  $Var_{ran}$ , as a function of the dimensionless time  $\tau$  grows slowly and is much smaller than the variance  $Var_{reg}$  in the case of the regular disorder (Fig.4.17).

*localization length*, does not grow with time ad infinitum.

Figure 4.20 shows that our position distributions  $P_t^{ran}(x; x_0)$  can be fit to a decaying exponential reasonably well; the localization length being 3.5 at  $\tau = 200$ . The time dependence of the width of the position distribution can be read off from Fig.4.19, i.e. from the time evolution of the variance, which grows slowly or perhaps even stops growing. Although our numerical results show only the time range  $\tau \in [0, 200]$  and are of limited accuracy, they support strongly our final conclusion: An  $e$  anyon living on a ladder-like lattice in a random environment of static  $m$  anyons *remains localized*, its motion is exponentially suppressed. As a consequence, the logical errors of the corresponding quantum memory are also exponentially suppressed — the time it takes for a logical error to occur is exponentially large in the size of the system.

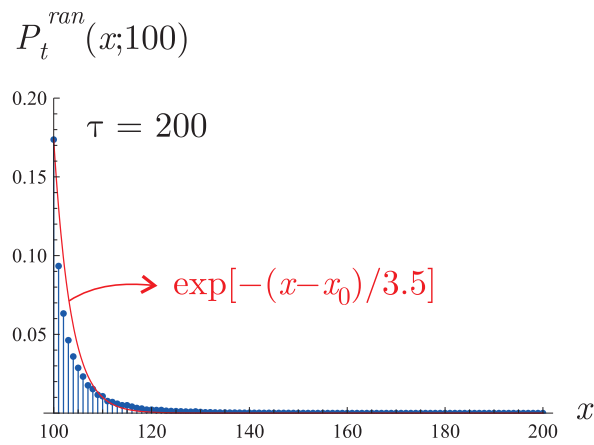


Figure 4.20: The position distributions  $P_t^{ran}(x; 100)$  can be fit to a decaying exponential. We show the fit for the “right wing” of the distribution at  $\tau = 200$ . The fit is  $e^{-\frac{x-x_0}{3.5}}$  up to a constant prefactor. The localization length is 3.5 in this case.

# Chapter 5

## Conclusion

We have reviewed the theory (Chapter 2) as well as the experimental aspects (Chapter 3) of two dimensional particles with exotic exchange statistics called anyons.

In the last chapter we investigated the propagation of anyons on the toric code to inspect the stability of this topological quantum memory. We used a simplified model defined on a strip with a ladder-like lattice. The evolution of a quantum particle (a continuous-time quantum walk) was exactly solved in one dimension for a finite cycle (4.51), an infinite line (4.61) and a finite cycle with disordered couplings between the neighboring vertices (4.94, 4.95) (they were allowed to take values  $+1$  or  $-1$ ). We showed that any disorder of the type under consideration leads to the same delocalization behavior as in the case of uniform coupling. Subsequently, we studied numerically the propagation of an anyon on the ladder lattice with disorder and compared two cases. When the disorder was regular, periodic, the particle delocalized (Fig.4.16 and 4.17). On the other hand, in the case of a random disorder, the Anderson localization effect took place and the anyon remained at its initial position (Fig.4.18 and 4.19). More precisely, its wave function decayed exponentially with the distance.

Hence, we have shown (in analogy with [7]) that a random disorder imprinted in a topological quantum memory can be used to improve its robustness against logical errors.

# Appendix A

## Braid group

Braids are formed when  $n$  points on a horizontal plane are connected by  $n$  strands to  $n$  points on another horizontal plane, parallel to the first one, directly below the first  $n$  points. The strings are not allowed to go back upwards at any point in their travel. Two braids are considered the same (or equivalent) if one can be transformed into the other via an ambient isotopy of the space (a continuous deformation that doesn't cross the strings) that fixes the endpoints of each string (Fig.A.1).

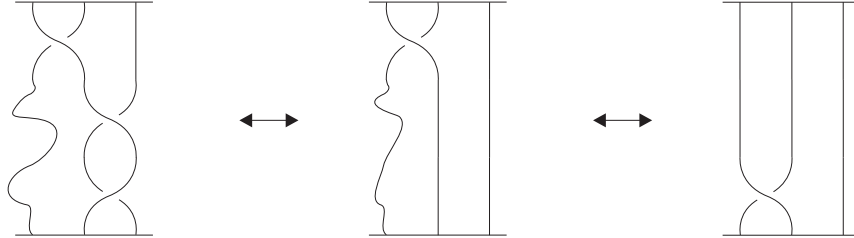


Figure A.1: An example of equivalent braids. One can be transformed into the other via an ambient isotopy of the space that fixes the endpoints of each string.

In order to describe a given braid we define the *braid group*. The braid group  $B_n$  of  $n$ -strand braids is a group generated by  $n - 1$  symbols  $\sigma_1, \dots, \sigma_{n-1}$  (depicted in Fig.A.2(a)) with the operation of concatenation (Fig.A.2(b)). The identity element is the diagram with “ $n$  straight lines” (Fig.A.3(a)) and the inverse of a generator  $\sigma_j$ , denoted  $\sigma_j^{-1}$ , has the type of crossing opposite from  $\sigma_j$  (Fig.A.3(b)).

The generators of the braid group satisfy two additional relations:

$$\sigma_i \sigma_{i+1} \sigma_i = \sigma_{i+1} \sigma_i \sigma_{i+1} \quad \text{for } i \in \{1, 2, \dots, n - 2\} , \quad (\text{A.1})$$

$$\sigma_i \sigma_j = \sigma_j \sigma_i \quad \text{for } i, j \in \{1, \dots, n - 1\}, |i - j| \geq 2 . \quad (\text{A.2})$$

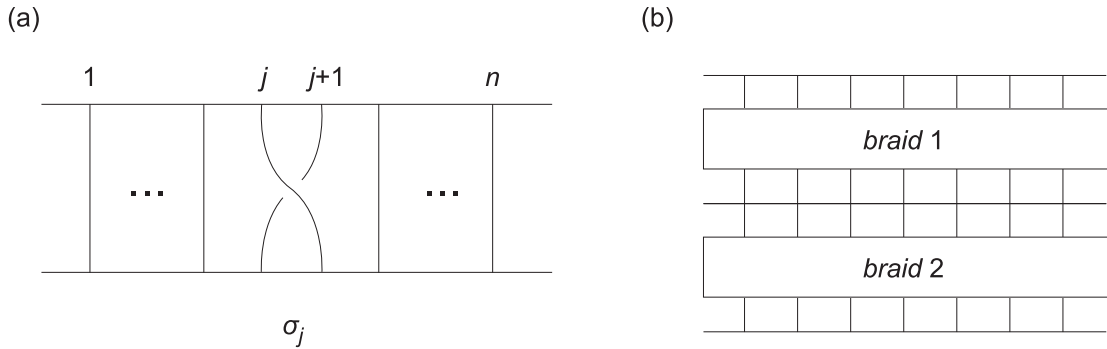


Figure A.2: (a) The generators  $\sigma_j$  of the braid group  $B_n$  ( $j$  runs from 1 to  $n - 1$ ). (b) The braid group operation of concatenation — one braid is put on top of the other and the corresponding strands are glued together.

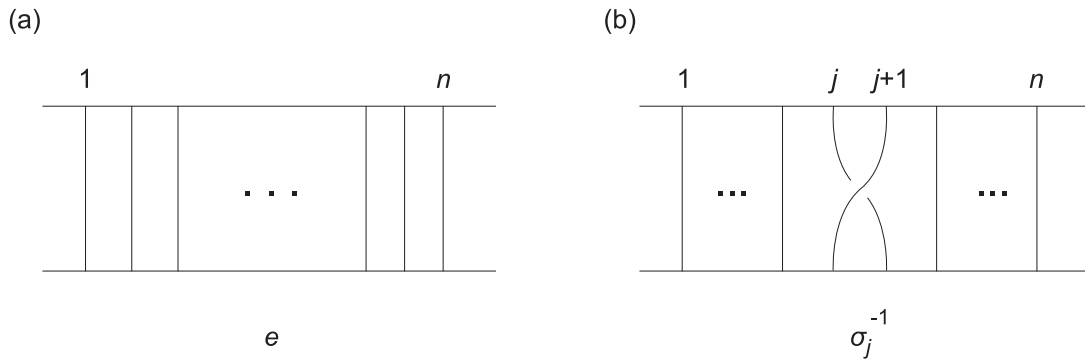


Figure A.3: (a) The identity element in the braid group  $B_n$ . (b) The inverses of the generators  $\sigma_j$  of  $B_n$ .

These relations are pictured in Figure A.4. The group relation  $\sigma_j^{-1}\sigma_j = \sigma_j\sigma_j^{-1} = 1$  together with the relations (A.1) and (A.2) guarantee that any two words in braid generators (and their inverses) represent the same braid if and only if they are the same element of  $B_n$ . These three relations correspond to the three Reidemeister moves — the three knot preserving transformations (for an introduction into the knot theory see e.g. [37]). This group approach to braids is due to Emil Artin [38] and therefore  $B_n$  is sometimes called the *Artin braid group*.

Physical relevance of the braid group is apparent from the following observation. Consider  $n$  indistinguishable particles in a plane (Fig.A.5), which we will identify with the complex plane  $\mathbb{C}$ , and assume two particles cannot occupy the same position. The config-

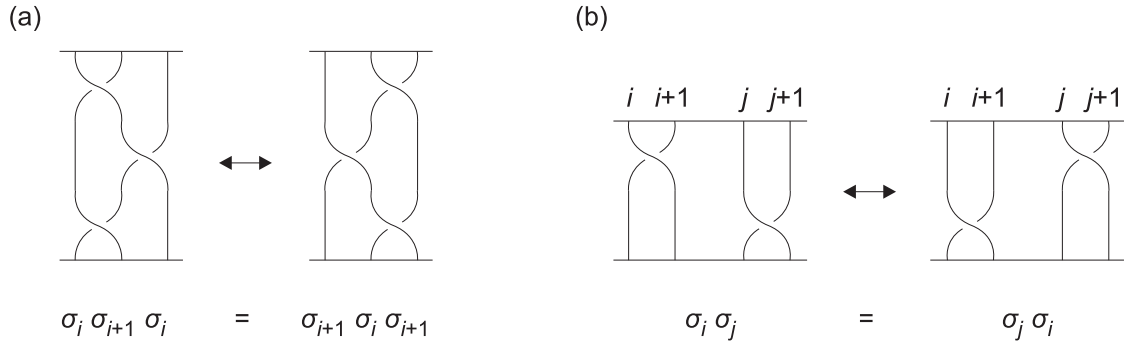


Figure A.4: The braid group relations: (a) represents the relation A.1 and (b) represents the relation A.2. The braid on the left hand side is the same as that on the right hand side.

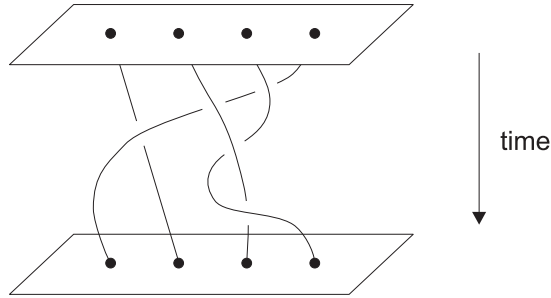


Figure A.5: Four indistinguishable particles in a plane evolving in time. As the particles move around one another, their worldlines in the 2+1 dimensional spacetime constitute a braid (provided that the initial and the final configuration is the same). The braid group  $B_4$  is the fundamental group of the space of four indistinguishable particles.

uration space of this physical system is

$$X = (\mathbb{C}^n \setminus \Delta) / S_n, \tag{A.3}$$

where  $\Delta = \{(z_1, \dots, z_n) \in \mathbb{C}^n \mid z_i = z_j \text{ for some } i \neq j\}$  and  $S_n$  is the permutation group of  $n$  symbols. As the particles move around in the plane, their worldlines trace curves in the 2 + 1 dimensional spacetime as depicted in Figure A.5. One can prove a plausible statement that the braid group  $B_n$  is the fundamental group of the space  $X$ , i.e.

$$B_n = \pi_1(X). \tag{A.4}$$

## A.1 Representations of the braid group

One-dimensional unitary representations of the braid group  $B_n$  are easy to classify. Let us assign complex numbers  $e^{i\alpha_j}$ ,  $\alpha_j \in [0, 2\pi]$ , to the generators  $\sigma_j$ . The relation (A.2) is clearly satisfied. The other braid group relation (A.1) translates into

$$e^{i\alpha_j} e^{i\alpha_{j+1}} e^{i\alpha_j} = e^{i\alpha_{j+1}} e^{i\alpha_j} e^{i\alpha_{j+1}} \quad \text{for } j \in \{1, 2, \dots, n-2\}, \quad (\text{A.5})$$

which enforces  $e^{i\alpha_1} = \dots = e^{i\alpha_{n-1}} \equiv e^{i\alpha}$ . The angle  $\alpha$  is the only parameter characterizing the particular representation

$$\rho_\alpha : \sigma_j \mapsto e^{i\alpha} \quad , \quad j \in \{1, 2, \dots, n-1\} . \quad (\text{A.6})$$

We can see that the representation  $\rho_\alpha$  is not faithful as it does not distinguish distinct braid group elements  $\sigma_j \sigma_{j+1}$  and  $\sigma_{j+1} \sigma_j$ . On the other hand, unlike the symmetric group  $S_n$ ,  $\rho_\alpha$  does tell apart the identity and the elements  $\sigma_j^2$  (provided that  $\alpha \neq 0, \pi$ ). In fact,  $S_n$  differs from  $B_n$  only by the additional requirement  $\sigma_j^2 = 1$ , which allows only two one-dimensional unitary representations  $\rho_+ : \sigma_j \mapsto 1$  and  $\rho_- : \sigma_j \mapsto -1$ .

The braid group representation theory in higher dimensions is much richer and much more complicated. It is connected with the polynomial invariants of knots. An interested reader is directed to [39] for an overview.

# Bibliography

- [1] J. Leinaas and J. Myrheim, “On the theory of identical particles,” *Il Nuovo Cimento B (1971-1996)*, vol. 37, pp. 1–23, 1977. 10.1007/BF02727953.
- [2] F. D. M. Haldane, ““fractional statistics” in arbitrary dimensions: A generalization of the pauli principle,” *Phys. Rev. Lett.*, vol. 67, pp. 937–940, Aug 1991.
- [3] A. Khare, *Fractional statistics and quantum theory*. World Scientific, 2005.
- [4] D. Arovas, J. R. Schrieffer, and F. Wilczek, “Fractional statistics and the quantum hall effect,” *Phys. Rev. Lett.*, vol. 53, pp. 722–723, Aug 1984.
- [5] A. Y. Kitaev, “Fault-tolerant quantum computation by anyons,” *Annals of Physics*, vol. 303, no. 1, pp. 2 – 30, 2003.
- [6] P. W. Anderson, “Absence of diffusion in certain random lattices,” *Phys. Rev.*, vol. 109, pp. 1492–1505, Mar 1958.
- [7] J. R. Wootton and J. K. Pachos, “Bringing order through disorder: Localisation of errors in topological quantum memories,” *ArXiv e-prints*, Jan. 2011.
- [8] R. Mirman, “Experimental meaning of the concept of identical particles,” *Il Nuovo Cimento B (1971-1996)*, vol. 18, pp. 110–122, 1973. 10.1007/BF02832643.
- [9] W. Massey, *A basic course in algebraic topology*. Graduate texts in mathematics, Springer-Verlag, 1991.
- [10] R. Fox and L. Neuwirth, “The braid groups,” *Mathematica Scandinavica*, vol. 10, p. 119, 1962.
- [11] E. Fadell and L. Neuwirth, “Configuration spaces,” *Mathematica Scandinavica*, vol. 10, p. 111, 1962.

- [12] R. Feynman and A. Hibbs, *Quantum mechanics and path integrals [by] R. P. Feynman [and] A. R. Hibbs*. International series in pure and applied physics, McGraw-Hill, 1965.
- [13] M. G. G. Laidlaw and C. M. DeWitt, “Feynman functional integrals for systems of indistinguishable particles,” *Phys. Rev. D*, vol. 3, pp. 1375–1378, Mar 1971.
- [14] W. Pauli, “The connection between spin and statistics,” *Phys. Rev.*, vol. 58, pp. 716–722, Oct 1940.
- [15] Y. Aharonov and D. Bohm, “Significance of electromagnetic potentials in the quantum theory,” *Phys. Rev.*, vol. 115, pp. 485–491, Aug 1959.
- [16] Z. Ezawa, *Quantum Hall effects: field theoretical approach and related topics*. World Scientific, 2008.
- [17] K. v. Klitzing, G. Dorda, and M. Pepper, “New method for high-accuracy determination of the fine-structure constant based on quantized hall resistance,” *Phys. Rev. Lett.*, vol. 45, pp. 494–497, Aug 1980.
- [18] E. H. Hall, “On a new action of the magnet on electric currents,” *American Journal of Mathematics*, vol. 2, no. 3, pp. 287 – 292, 1879.
- [19] D. C. Tsui, H. L. Stormer, and A. C. Gossard, “Two-dimensional magnetotransport in the extreme quantum limit,” *Phys. Rev. Lett.*, vol. 48, pp. 1559–1562, May 1982.
- [20] R. B. Laughlin, “Anomalous quantum hall effect: An incompressible quantum fluid with fractionally charged excitations,” *Phys. Rev. Lett.*, vol. 50, pp. 1395–1398, May 1983.
- [21] A. Stern, “Anyons and the quantum hall effect—a pedagogical review,” *Annals of Physics*, vol. 323, no. 1, pp. 204 – 249, 2008. January Special Issue 2008.
- [22] A. Bohm, A. Mostafazadeh, H. Koizumi, Q. Niu, and J. Zwanziger, *The Geometric Phase in Quantum Systems: Foundations, Mathematical Concepts, and Applications in Molecular and Condensed Matter Physics*. Theoretical and Mathematical Physics Series, Springer, 2010.
- [23] M. V. Berry, “Quantal phase factors accompanying adiabatic changes,” *Proceedings of the Royal Society of London. A. Mathematical and Physical Sciences*, vol. 392, no. 1802, pp. 45–57, 1984.

- [24] B. Simon, “Holonomy, the quantum adiabatic theorem, and berry’s phase,” *Phys. Rev. Lett.*, vol. 51, pp. 2167–2170, Dec 1983.
- [25] Y. Aharonov and J. Anandan, “Phase change during a cyclic quantum evolution,” *Phys. Rev. Lett.*, vol. 58, pp. 1593–1596, Apr 1987.
- [26] A. Lerda, *Anyons: quantum mechanics of particles with fractional statistics*. Lecture notes in physics: Monographs, Springer-Verlag, 1992.
- [27] F. Wilczek, *Fractional statistics and anyon superconductivity*. World Scientific, 1990.
- [28] S. Spielman, K. Fesler, C. B. Eom, T. H. Geballe, M. M. Fejer, and A. Kapitulnik, “Test for nonreciprocal circular birefringence in  $yba_2cu_3o_7$  thin films as evidence for broken time-reversal symmetry,” *Phys. Rev. Lett.*, vol. 65, pp. 123–126, Jul 1990.
- [29] P. W. Shor, “Polynomial-time algorithms for prime factorization and discrete logarithms on a quantum computer,” *SIAM Review*, vol. 41, no. 2, pp. 303–332, 1999.
- [30] P. Shor, “Fault-tolerant quantum computation,” *Foundations of Computer Science, Annual IEEE Symposium on*, vol. 0, p. 56, 1996.
- [31] D. Gottesman, “Class of quantum error-correcting codes saturating the quantum hamming bound,” *Phys. Rev. A*, vol. 54, pp. 1862–1868, Sep 1996.
- [32] A. R. Calderbank, E. M. Rains, P. W. Shor, and N. J. A. Sloane, “Quantum error correction and orthogonal geometry,” *Phys. Rev. Lett.*, vol. 78, pp. 405–408, Jan 1997.
- [33] E. Dennis, A. Kitaev, A. Landahl, and J. Preskill, “Topological quantum memory,” *Journal of Mathematical Physics*, vol. 43, no. 9, pp. 4452–4505, 2002.
- [34] C. A. Mueller and D. Delande, “Disorder and interference: localization phenomena,” *ArXiv e-prints*, May 2010.
- [35] D. ben Avraham, E. Boltt, and C. Tamon, “One-dimensional continuous-time quantum walks,” *Quantum Information Processing*, vol. 3, pp. 295–308, 2004. 10.1007/s11128-004-9420-8.
- [36] I. Gradshteyn, I. Ryzhik, A. Jeffrey, and D. Zwillinger, *Table of integrals, series and products*. Academic Press, Academic, 2007.
- [37] C. Adams, *The knot book: an elementary introduction to the mathematical theory of knots*. American Mathematical Society, 2004.

- [38] E. Artin, “Theory of braids,” *The Annals of Mathematics*, vol. 48, pp. 101 – 126, 1947.
- [39] J. S. Birman and T. E. Brendle, “Braids: A Survey,” *ArXiv Mathematics e-prints*, Sept. 2004.